

# CHALMERS



## PREDICTIVE ENERGY MANAGEMENT FOR A MILD HYBRID LONG HAUL TRUCK

MASTER OF SCIENCE THESIS

MATTHIAS JÖNSSON

MILEN KOURTEV

*Department of Signals and Systems*  
CHALMERS UNIVERSITY OF TECHNOLOGY  
Göteborg, Sweden

EXE01/2010



# Abstract

The purpose of this thesis has been to analyze the potential of improved fuel economy of a mild-hybrid long-haul truck by use of preview-based energy-management control algorithms. Information regarding the road topography ahead of the vehicle enables improvement of the control of the energy distribution between the internal combustion engine and the electric motor for hybrid vehicles.

Three predictive energy management strategies have been developed. The functionality of these predictive energy management strategies were compared to the non-predictive energy management strategy used by Volvo powertrain in the mild-hybrid long-haul-truck project. The development of the predictive energy management strategies were performed inside the Global Simulations Platform (GSP), a simulation platform based on MATLAB/Simulink and used for full-vehicle simulations within the Volvo Group.

The potential to save fuel by predictive control mainly depends on the topography of the road. The mild hybrid only charges the battery by brake power recuperation, which means that the hybrid system is not used when the road is flat and no braking occurs. On hilly roads, non-predictive control can lead to saturations of the battery of the hybrid system. By knowing the present level of state-of-charge in the battery and the amount of recuperable energy ahead of the truck, the battery capacity can be used more efficiently. Our vehicle simulations showed that the predictive strategies can reduce the saturation of the battery by 50 % and give fuel savings of up to 0.2 percent on the Borås-Landvetter-Borås drive-cycle, compared to the non-predictive strategy used. The amount of fuel that can be saved on a certain drive-cycle depends on the size of the electric motor and the battery capacity of the hybrid system.

**KEYWORDS:** Hybrid Electric Vehicle HEV, Hybrid system, Diesel-electric hybrid, Electric machine EM, Regenerative, Recuperation, Fuel consumption, Prediction, Energy Management, Powertrain control, Equivalent Energy Management Strategy ECMS, State Of Charge SoC.

# Preface

First of all we would like to express our deepest thanks to our supervisor Lars Johannesson. Without his guidance, encouragement and bright ideas this thesis would not have been the same . We would also like to thank one of our supervisors at Volvo, Mikael Lellky, who made it possible for us to attend for this master thesis and who sat with us for many hours while helping us out with Matlab/Simulink. His skills within this area have been of big importance for us. A special thanks also goes to Lotta Holmberg and to Jonas Hellgren. Lotta has helped us with everything from administrative work and paper filling, to reviews of our paper. Jonas have contributed with his knowledge and expertise in the field of control theory and optimization.

We would also like to thank our examiner, Bo Egardt.

Many thanks also go to all the co-workers at Volvo who got involved with this project, for all their friendliness and for making the time at Volvo memorable for us as well as to friends and family from home who have supported a lot. From Milen: a very special thank to you Eva-Britt, for all your help and support with everything- it was of much value for me.

Göteborg, June 20, 2011

MATTHIAS JÖNSSON AND MILEN KOURTEV



# CONTENTS

Preface .....	vii
<b>1 Introduction</b>	<b>1</b>
1.1 Objective .....	4
1.2 Outline .....	4
<b>2 Notation</b>	<b>5</b>
<b>3 Background</b>	<b>6</b>
3.1 Modeling the Dynamics of the Vehicle .....	6
3.2 Global Simulation Plattform and VSim+ .....	8
3.3 Drive cycles .....	8
3.4 e-Horizon and estimation of future road data .....	10
<b>4 The hybrid truck model</b>	<b>11</b>
4.1 Parallel hybrid .....	11
4.2 Electric storage system .....	12
4.3 Internal Combustion Engine .....	13
4.4 Electric motor .....	15
4.5 Engine Electronic Control Unit .....	15
4.6 The truck model .....	15
4.7 Torque distribution .....	17
<b>5 Optimization</b>	<b>19</b>
5.1 Optimal control .....	19
5.2 Equivalent Consumption Minimization Strategy .....	21
<b>6 The non-predictive energy management strategy</b>	<b>24</b>

6.1	Non-predictive equivalence factor .....	24
<b>7</b>	<b>Predictive energy management</b>	<b>28</b>
7.1	Introductory theory .....	28
7.1.1	Predicted recuperation .....	29
7.1.2	Overspeed .....	29
7.2	Predictive Reference Signal Generator .....	31
7.2.1	Introduction to the pRSG strategy .....	31
7.3	Constructing the Reference Trajectory .....	32
7.3.1	Segments .....	32
7.3.2	Implementating the pRSG .....	35
7.4	Telemetry Equivalent Consumption Minimization Strategy .....	37
7.5	Constrained T-ECMS .....	39
<b>8</b>	<b>Results</b>	<b>42</b>
8.1	Fuel consumption .....	42
8.2	Tunable parameters .....	42
8.3	Drivability .....	43
8.4	Effects from changes in the e-Horizon length .....	46
<b>9</b>	<b>Discussion</b>	<b>48</b>
9.1	Fuel consumption .....	48
9.2	Parameters .....	48
9.3	Horizon change .....	49
<b>10</b>	<b>Future work</b>	<b>51</b>
	APPENDIX	<b>57</b>
A	Fuel consumption Results	<b>57</b>

---

B	Change in the average vehicle speed	<b>59</b>
C	Tuning of the T-ECMS and pRSG parameters	<b>61</b>
	C.0.1 Defining the range of the parameters .....	62
D	Drive cycles	<b>65</b>
E	Series hybrid	<b>69</b>



# List of Figures

3.1	Figure of the main forces affecting the truck. . . . .	6
3.2	The simulation platform. The figure shows the topmost level of the simulation platform, which consists of a truck chassis model, a driver model and the road environment (drive cycle). These models are built up by several subsystems. . . . .	9
3.3	Abbreviations for the three drive-cycles. . . . .	9
3.4	A road-map example. The figure shows a few data points taken from a road map. The columns, read from left to right, give the distance from the starting position, the speed that has to be hold and the altitude of the road in meters above sea level, respectively. . . . .	10
4.1	Full parallel hybrid configuration. B: battery, E: engine, M: motor, P: power converter, T: transmission (including clutch and gears), V: axles and vehicle. Bold lines: mechanical link, solid lines: electrical link. . . . .	12
4.2	Mild parallel hybrid configuration. B: battery, E: engine, M: motor, P: power converter, T: transmission (including clutch and gears), V: axles and vehicle. Bold lines: mechanical link, solid lines: electrical link. . . . .	12
4.3	Energy density of different on-board energy storage sources. The blue bars indicate the actual chemical energy available and the orange bars represent the energy that will be available at the wheels when energy losses from the combustion and the powertrain are considered. . . . .	13
4.4	Illustration of the state of charge and the definition of state of charge window. . . . .	13
4.5	SoC-level example for the BLB drive-cycle. This is an illustration of how the SoC changes within the ESS throughout the drive-cycle. These kind of plots give a good overview of how the energy within the ESS is used and will be used in the sequel of this paper to compare and analyze results from the different energy management strategies. . . . .	14
4.6	An ICE motor-map example from GSP. The left-most column and the upper-most row together define the desired operating point, declaring the demanded output-torque, $T$ , and engine speed, $\omega$ , respectively. The output is given as the fuel-mass flow rate, $\dot{m}_f$ . . . . .	14

4.7	An EM motor-map example. The left-most column and the upper-most row together define the desired operating point, declaring the demanded output-torque, $T$ , and engine speed, $\omega$ , respectively. The output is given as the efficiency of the EM, $\eta^{EM}$ , at that operating point. ....	15
4.8	Different parameters that were used in simulations of the truck. The mass was hold constant. ....	16
4.9	Schematic of the truck model. ....	16
5.1	Graphical view of the ECMS look-up table. The graph shows the optimal EM torques, $\tilde{T}_{EM}$ , for a range of torque demands, $T_{DEM}$ , and equivalence factors. The engine speed, $\omega$ , is in this case 1200 rpm. ....	23
6.1	Illustration of the equivalence factor function. The SoC-window is on the x-axis while the equivalence values are presented on the y-axis. . .	24
6.2	SoC-curve for the BLB drive cycle using the non-predictive energy management system. The strategy is to deplete the ESS from energy as fast as possible to avoid an under-used hybrid system. ....	25
6.3	Illustration for the effect of manipulating the $Rt_{SOCRef}$ parameter. Changing this parameter will make the transition between the balance value and the end values smoother. ....	26
6.4	Illustrates the effect of manipulating the $Kp_{SOCRef}$ parameter. It is seen that the gradient of the balance value is changed when altering this parameter. ....	26
6.5	Illustrates the effect of manipulating the $Rt_{WeightRef}$ parameter. This decides the level of the balance value and simulations shows that it has a more substansial effect on the fuel consumption than the other two parameters. ....	26
7.1	Over-speed example. The set-speed (lower line, upper graph) is constant on 85 km/h while the actual speed goes up to 90 km/h. Braking(lower graph, green line) does not occur until the actual speed has reached the set-speed plus the over-speed value at 90 km/h. ....	30
7.2	Illustrates for the effects of over-speed versus recuperation. It is seen that recuperation is not happening (red line) unless the actual speed has reached 90 [km/h]. ....	30
7.3	Illustration of the idea behind knowledge of future information about the road topography. In figure the position point is the truck current position and the longitudinal line is the end of the e-horizon interval. ....	31

7.4	Synthesis of the reference signal. $SoC_0$ is the present $SoC$ level at present position. From this position an optimization of every free segment is made based on the information of $\Delta SoC$ in the fixed segments matrix $FIX$ . The area between $SoC_{min}$ and $SoC_{max}$ is the $SoC$ window. The unknown variable is $SoC_i$ which is decided with the estimate $\Delta \hat{SoC}_i$ . $\Delta \hat{SoC}_i$ is basically the slope of the free segment trajectory . . . . .	33
7.5	Illustration of the implementation of pRSG-ECMS. In this case the P-controller is included inside the ECMS-block. The x-signal is the SoC-trajectory with which the P-controller calculates an equivalence factor which, together with the present torque demand and the engine speed, will be the input to the ECMS algorithm. . . . .	35
7.6	This is a figure that illustrates mode 1. . . . .	36
7.7	This is a figure that illustrates mode 2 (recuperation mode) with constant slope (mode 1). It is seen in figure that when the $SoC_{ref}$ -value (blue line) is above the $SoC$ -value the slope is in mode 1 as long as there are no recuperation detected in e-horizon . . . . .	36
7.8	Example of how the equivalence factor is adjusted by the T-ECMS strategy. In the top-most graph the blue line represents the energy that is needed to contribute to the wheels ( $E_m(t)$ ) and the green line represents the amount of recuperable energy. The middle graph shows the SoC-curve for the specific drive cycle and the bottom graph shows the resulting equivalence factor. These results are from a simulation on the BLB drive-cycle with a 120 kW EM and 0.6 kWh ESS. . . . .	38
7.9	Resulting SoC-curve for low values of $S_{dis}$ and $S_{chg}$ . The curve reaches the upper boundary of the SoC-window 4 % of the time and the lower boundary 46 % of the time. These results are from a simulation on the BLB drive-cycle with a 120 kW EM and 0.6 kWh ESS. . . . .	39
7.10	Resulting SoC-curve for an optimal choice of the $S_{dis}$ and $S_{chg}$ values. The curve reaches the upper boundary of the SoC-window 6 % of the time and the lower boundary 20 % of the time. These results are from a simulation on the BLB drive-cycle with a 120 kW EM and 0.6 kWh ESS. . . . .	40
7.11	Resulting SoC-curve for high values of $S_{dis}$ and $S_{chg}$ . The curve reaches the upper boundary of the SoC-window 19.14 % of the time and the lower boundary 0 % of the time. These results are from a simulation on the BLB drive-cycle with a 120 kW EM and 0.6 kWh ESS. . . . .	40

7.12	The blue line (a) represents the actual SoC-level. The red line (b) represents the resulting SoC-trajectory if an equivalence factor that is higher than the pRSG-strategy outputs is used. The yellow line (d) is the SoC-trajectory achieved by using the equivalence factor from the pRSG strategy. The green line (c) is a resulting SoC-trajectory if a lower equivalence factor than the pRSG outputs is used. . . . .	41
8.1	Amount of fuel that is saved by using hybrid systems on the different drive-cycles. The rows give the amount of fuel that is saved in percent by using the different energy management systems relative to the conventional truck, where the upper row is the non-predictive energy management strategy already in use by Volvo and the three lower rows are the predictive energy management strategies. . . . .	42
8.2	The bars indicate the amount of fuel that can be saved by using predictive energy management strategies, compared to the non-predictive strategy. All values yield for the hybrid configuration with a 120 kW motor and a 1.35 kWh battery capacity. . . . .	43
8.3	Optimal tunable parameters for the hybrid set-up with a 120 kW and 1.35 kWh battery capacity. . . . .	43
8.4	Amount of time the actual speed is at least 3 [km/h] below the set-speed. . . . .	45
8.5	Percentual difference with at least 3 [km/h] beneath the set-speed and average road gradient. It can be seen that the average road gradient has a big influence on the amount of time that the vehicle spends at lower speeds than the set-speed. . . . .	45
8.6	Example of speed-loss at uphill. When the truck starts driving at steep uphill it is affected by a speed-loss. . . . .	46
8.7	The set-speed and the average speeds achieved by the trucks for the different drive-cycles. The hybrid trucks have a hybrid set-up with a 1.35 [kWh] battery and a 120 [kW] EM. . . . .	46
8.8	Fuel savings using the pRSG strategy with two different preview lengths. Comparisons are relative to the non-predictive algorithm. . .	47
9.1	Average road gradients and achieved fuel savings on different drive-cycles. Comparisons are made on the conventional truck. . . . .	48
9.2	The left-most bar indicate the amount of fuel that is saved when the electric motor is held constant and the ESS capacity is changed. The right-most bar indicate how the fuel economy is affected by changing the maximum input and output power from the EM. All values are taken for the BLB drive-cycle and the comparisons are made with a conventional truck. . . . .	49

9.3	Fuel savings when using optimal and average tunable parameters. All values are taken from a hybrid set-up with a 120 kW motor and a 1.35 kWh battery capacity. Comparisons are made on the non-predictive energy management strategy. ....	50
9.4	The bars indicate the amount of fuel that is saved compared to the non-predictive strategy by using the pRSG strategy with preview horizons of 3 kilometers and 6 kilometers. A preview horizon of 6 kilometers give better results on all three drive-cycles. ....	50
A.1	Fuel savings achieved by using the pRSG strategy compared to a conventional truck and a hybrid truck using the present non-predictive energy management strategy. ....	57
A.2	Fuel savings achieved by using the T-ECMS strategy compared to a conventional truck and a hybrid truck using the present non-predictive energy management strategy. ....	58
A.3	Fuel savings achieved by using the CT-ECMS strategy compared to a conventional truck and a hybrid truck using the present non-predictive energy management strategy. ....	58
B.1	Average speeds for for a conventional truck and trucks using the different energy management strategies. The four different row-sections define the degree of hybridization where the row-section from top to bottom represents the following; 60 kW EM and 0.6 kWh ESS, 120 kW EM and 0.6 kWh ESS, 60 kW EM and 1.35 kWh ESS, 120 kW EM and 1.35 kWh ESS. ....	59
C.1	A tuning example. The blue line is the total fuel consumption for the BLB drive cycle using a 1.35 kWh battery and 120 kW EM. The line was built up by 96 different parameter combinations between $S_{dis}$ and $S_{chg}$ . The red ellipse represents a local minimum around which further and more narrow tunings were made with a smaller step-size, $\Delta$ . The red line represents the fuel consumption for the conventional vehicle and the green line represents the fuel consumption resulted from the non-predictive hybrid truck. ....	61
C.2	Optimal parameters for the T-ECMS strategy. ....	62
C.3	Optimal parameters for the pRSG strategy. ....	63
C.4	SoC-curve over the BLB drive-cycle with the T-ECMS strategy. Parameters are much lower than the balancing factor of the equivalence factor. ....	63
C.5	SoC-curve over the BLB drive-cycle with the T-ECMS strategy. Parameters are much higher than the balancing factor of the equivalence factor. ....	64

---

D.1	Altitude and set-speed for the Borås-Landvetter-Borås (BLB) drive cycle. ....	66
D.2	Altitude and set-speed for the Paris-Lille (PL) drive cycle. ....	66
D.3	Altitude and set-speed for the Frankfurt-Koblenz (sx135) drive cycle. ....	67
E.1	Basic series hybrid configuration. B: battery, E: engine, G: generator, M: motor, P: power converter, T: transmission (including clutch and gears), V: axles and vehicle. Bold lines: mechanical link, solid lines: electrical link. ....	70

# 1 Introduction

One of the most important problems today is the steadily deteriorating world climate. This deterioration is a result of a large, and still increasing, energy usage which is mostly based on non-renewable energy resources such as oil, coal and other fossil fuels [12], [20]. In 2007 it was estimated that fossil fuels amounted to an 86.4 percent share of the total primary energy consumption in the world [42]. Fossil fuels come from resources that have arisen by anaerobic decomposition of buried dead coal-based organisms, such as dead plants and animals. This process is slow and the age for most of the fossil fuels is typically millions of years but can also exceed 650 million years [36].

Energy is retrieved from the fossil fuel by oxidation as a result from burning. During such oxidation green house gases, primarily carbon dioxide, are produced. About 21.3 gigatonnes of carbon dioxide is produced each year by burning fossil fuel, but it is estimated that natural processes only can absorb half of that amount, leading to a net increase of carbon dioxide in the atmosphere [33]. This net-increase of green-house gases in the atmosphere is said to be the cause of the global warming [34, 39, 1, 35, 41].

There are several reasons to reduce the usage of fossil fuels and replace them with alternative sustainable energy resources or to find technologies with increased energy efficiency. One of these reasons is to reduce the anthropogenic climate impact which was mentioned earlier<sup>1</sup> [25]. Another reason is that reserves of fossil fuel are being depleted at a much higher rate than new ones are being made as a result of the high energy consumption and the long process-time of the anaerobic decomposition.

When it comes to diesel engine exhaust another concern is the emission of *diesel particulate matter* (DPM), which is also referred to as *diesel exhaust particles* (DEP). These particles are so called *ultrafine particles* (UFP) which are in the nano-scale range of less than 100 nanometers and pose a health risk while they can penetrate deep into the lungs [10]. These particles are not easily removed from the body and can give rise to lung diseases and various inflammatory symptoms [6, 22, 30]. The rough surface of these particles makes it easy for other toxins in the environment to bind to them, making the risk even higher [31, 26]. In 2001 the mortality of the German population (82 million people) was at least 14400 because of diesel soot exposure [46, 47]. Fueled by the increasing fossil fuel usage and the rise of new nano-materials which range in the UFP-scale there has been an increasing concern about UFPs and how to regulate the emissions of these particles even more [45, 7, 8, 9, 44, 21].

One promising technology for reducing the fuel consumption in vehicles is the *hybrid technology*. A hybrid vehicle needs to have at least two power sources, usually a

---

<sup>1</sup>Anthropogenic climate change refers to the production of greenhouse gases emitted by human activity.

fossil fuel-based energy source and an electric- or kinetic energy source, which fuel the prime mover/movers of the vehicle.

A *hybrid electric vehicle* (HEV) combines conventional internal combustion engine (ICE) propulsion together with an electric propulsion system, usually an electric motor (EM). An HEV has both a fossil fuel-based energy source and an electric storage system (ESS), usually a battery or supercapacitor [23]. The main purpose of this combination is either to save fuel or to get better performance, compared to a conventional vehicle. By using *regenerative braking* the kinetic energy of the vehicle that otherwise would disappear as heat in the brakes while braking can be regenerated, or *recuperated*, into the battery. The recuperated energy can later be used to drive the EM in order to either propel the whole vehicle by itself, or to support the ICE [19].

The first gasoline-electric hybrid automobile in the world was developed already in 1900 when Ferdinand Porsche developed the Lohner-Porsche Mixte Hybrid [?, ?]. Due to different factors the interest for HEVs was low for a long time since then. It was not until the mid 1980s that the interests for these kinds of systems grew and since the start of year 2000 there has been more of an explosion around the development of these kind of systems. The fuel savings within an HEV emerge from two main reasons [40]:

1. An HEV can recuperate some of the kinetic energy while braking and store it for later use.
2. Optimal operating points within the electric motor and especially the ICE can be reached by combining the power from both of the propulsion systems.

The amount of fuel that can be saved depends on the size of the EM and the battery capacity, the road dynamics and the control algorithm used for the energy management within the hybrid system.

A common classification that is made on the HEVs is how the power is supplied to the powertrain. There are three main types for the power supply within an HEV, and these are the *series hybrid vehicle*, the *parallel hybrid vehicle*, and the *combined hybrid vehicle*. In case of the parallel HEVs a classification regarding the amount of hybridization is made as well and the two main classifications are the *mild parallel hybrid* and the *full parallel hybrid*, where the mild parallel vehicle has a power output from the EM that is not sufficient to drive the whole vehicle on its own. In case of the full hybrid the vehicle can be propelled by either the EM or the ICE alone.

The Volvo Group Corporation has been using hybrid technologies in shuttle buses and waste disposal units. The group is now developing a hybrid system for *long haul trucks* as well. These trucks usually hold constant speed for long distances without braking so there will be much less recuperation phases involved and therefore the impact of using hybrid technology can be assumed to be less on such vehicles.

---

Nevertheless these vehicles usually carry heavy cargoes and drive for very long distances which lead to high total fuel consumption rates. For a haulage contractor company with many such vehicles even a small decrease in fuel consumption would lead to high economical savings. Until the date of writing the Volvo Group has use non-predictive strategies to control the hybrid system. These strategies depend on present, or past, information about the vehicle and the road environment.

The Volvo Group has developed a system, ADAS RP, which finds the position of the truck by using various positioning systems and an onboard map and then calculates the probability for which routes the driver is most likely to drive up to a certain distance ahead of the present position. The Volvo Group is now testing which kind of technologies that may use this information within their trucks. After good initial results from the long haul HEV project they decided to investigate if the HEV control system could be further enhanced by using the prediction. The prediction consists of data regarding the road topography and set-speed up to a certain distance ahead of the truck, called the *e-Horizon length*. Within this thesis two distinct e-Horizon lengths of 3- and 6 kilometers were used.

The main benefit of using data that shows not only the present road conditions, but also road conditions ahead of the vehicle, is that the control of the interaction between the ICE and EM can be further enhanced. While the energy level in the ESS directly depends on the usage of the EM it will also be possible to enhance the usage of the ESS. In this work three different strategies were developed which use prediction-based optimization techniques to control the hybrid system. These strategies were the *Predictive Reference Signal Generator* (pRSG) [3] which was based on linear programming, the *Telemetry Equivalent Consumption Management Strategy* (T-ECMS) [2, 40], and the *Constrained T-ECMS* (CT-ECMS). The main objective was to see if the fuel consumption of a long haul HEV could be further decreased by using prediction. The purpose of the three methods was to lower the fuel consumption basically in two steps:

1. By decreasing losses between the ICE, the EM and the battery.
2. By enhancing the use of the battery. This is usually done by avoiding saturations of the battery.

One thing that all of the three prediction based algorithms have in common is the *Equivalent Consumption Management Strategy* (ECMS) [23], [3], which corresponds to the first item above. This strategy is also used by the present controller that is already available within Volvo hybrid trucks. The improvement of using prediction comes therefore from item two above, that is, by enhancing the usage of the battery. The three different prediction based strategies differ in how they avoid these saturations. All results were tested against the results from both a conventional, non-hybrid, truck as well as against the present non-predictive control strategy. Interestingly, one of the simplest predictive algorithms was also the one that was most efficient in lowering the fuel consumption for the routes used within this work.

## 1.1 Objective

The objective of this masters thesis is to develop, and to study the impact of, energy management strategies within a parallel diesel-electric mild hybrid long haul truck that use predicted data up to a given distance ahead of the truck. The aim is to further optimize the torque-split between the ICE and the EM, which is controlled by the engine electric control unit (EECU), in such a way that the fuel consumption is reduced. This is done by improving the usage of the electric storage system (ESS) in such a way that the saturations at the upper boundary of the State of Charge (SoC) window are minimized.

The development is carried out in the MATLAB®/Simulink®environment and the Global Simulation Platform (GSP). The simulation results of the energy management strategies are validated and a robustness test is performed. An extended study of how the performance and drivability of the truck are affected by the prediction-based energy management systems is done. Simulation results will be tested against both a conventional non-hybrid truck and against a hybrid truck using an existing energy management strategy that is not based on future road data.

## 1.2 Outline

In chapter one the objectives and background of this thesis are given. This chapter explains why the subject is of importance and summarizes the whole thesis and the main results. Chapter two presents the technical notations used. Chapter three presents the force equations that are affecting the vehicle and an overview of the simulation platform and the technology used for prediction is given. Chapter four presents the vehicle used within the simulation environment and explains the components involved in the hybrid system and how the power-flow can be modeled. Chapter five presents the underlying optimization algorithm that is used for both the predictive and non-predictive energy management systems. This optimization algorithm is used to calculate the optimal control signal for given operating points. Chapter six presents the existing, non-predictive, energy management strategy that has been developed by Volvo and is used at present time. Chapter seven gives a presentation and the theoretical background of the three predictive energy management strategies that were developed within this master thesis. This chapter is in large based on the theories given in chapter three and five. In chapter eight the results and analysis of the predictive energy management strategies is given and benchmarked against the results from the existing non-predictive energy management strategy that is already in use and that was explained in chapter six. In chapter nine the results from chapter eight are analyzed and followed by a discussion. In chapter ten guidelines are given for areas in which further studies or work can be carried out in order to improve the fuel efficiency of the truck even more.

## 2 Notation

### *Abbreviations*

ADAS-RP	Advanced Driver Assistance System Research Platform
BLB	Borås-Landvetter-Borås drive cycle
CT-ECMS	Constrained Telemetry equivalent Consumption management strategy
DOF	Degree of Freedom
e-Horizon	Electronic horizon
EAUX	Electric Auxiliaries
ECMS	Equivalent consumption management strategy
ECU	Electronic Control Unit
EECU	Engine Electronic Control Unit
EM	Electric motor
ESS	Electric Storage System
GBX	Gearbox
ICE	Internal combustion engine
HEV	Hybrid Electric Vehicle
MAUX	Mechanical Auxiliaries
PL	Paris-Lille drive cycle
pRSG	Predictive reference signal generator
SoC	State of Charge
sx135	Frankfurt-Koblenz drive cycle
T-ECMS	Telemetric equivalent Consumption management strategy

### *Capital Letters*

$T_{Dem}$	Torque demanded at the wheels ( $Nm$ )
$T_{EM}$	Torque delivered from or to the EM ( $Nm$ )
$T_{ICE}$	Torque delivered from the ICE ( $Nm$ )
$T_{tot}$	Total torque delivered from both ICE and EM ( $Nm$ )

### *Small Letters*

$\hat{m}_f$	Fuel mass flow
$v_{set}$	Set speed ( $km/h$ )
$s_{dis}$	Upper value of the equivalence factor
$s_{chg}$	Lower value of the equivalence factor
$SoC$	Present SoC reference value (%)
$\Delta\hat{SoC}$	Predicted slope reference value (%)

## 3 Background

In this chapter some background theory will be presented that is essential for the understanding of the later chapters. At first the mathematics of how to model the forces acting on the vehicle will be given. These calculations will be used when predicting the forces that will be acting on the truck for the prediction based control algorithms given in chapter 7. This will be followed by an introduction to the simulation environment that is used at Volvo, the drive cycles used within this thesis work and the technology behind the predictive data.

### 3.1 Modeling the Dynamics of the Vehicle

To make predictive hybrid energy management systems a model of the truck is needed which describes the dynamics of the vehicle when in movement. The model can be used to calculate, as well as to predict<sup>1</sup>, the most significant forces acting on the truck and the vehicle speed.

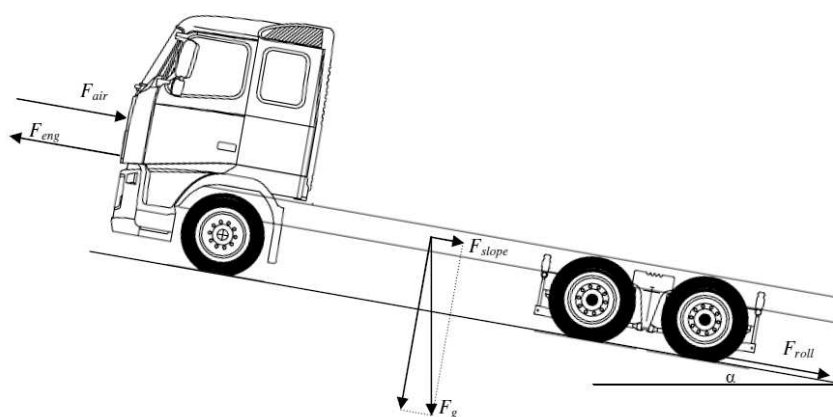


Figure 3.1. Figure of the main forces affecting the truck.

Five forces are considered in the truck model. The first one is the propelling force, which is the force delivered by the propulsion systems. Then there are three resistive forces that are counteracting the movement of the vehicle, and these are; the air resistance force, the resistive force between the wheels and the road and the internal friction forces within the truck that arise due to rotating parts in the engine. The last force is the gravitational force which counteracts the vehicle movement in upward slopes and accelerates the vehicle in downward slopes. With these forces the following balance equation based on Newton's second law [17] is derived,

---

<sup>1</sup>Given that future data, such as road topography, is given.

$$ma = F_{prop} - (F_{air} + F_{roll} + F_{grav} + F_{fric}), \quad (3.1)$$

where  $F_{air}$  is the air resistance force,  $F_{roll}$  is the rolling resistance force which arises from the friction between the wheels and the road,  $F_{fric}$  is the internal friction,  $F_{prop}$  the propelling force from the vehicle powertrain and  $F_{grav}$  is the gravitational force [19], [3].

The air resistance-force which affects the truck chassis when it moves through the air-medium is modeled by taking the aerodynamic coefficient,  $c$ , times the square of the truck's velocity  $v$ ,

$$F_{air} = c_{air}v^2. \quad (3.2)$$

Here  $c$  contains the two parameters, air density  $\rho$  and the frontal area  $A$  of the truck [3]. The coefficient  $c$  is assumed to be constant in order to simplify the behavior of the air resistance force. Since the vehicle speed is squared, the speed has a major impact on the air-resistance force.

The equation for the rolling resistance can be expressed as [19],

$$F_{roll} = c_{roll}mg \cos(\phi) \approx c_{roll}mg, \quad (3.3)$$

where  $c_{roll}$  is the rolling friction constant,  $m$  is the vehicle mass,  $g$  is the gravitational constant and  $\phi$  is the present road gradient [rad]. The road gradient is here assumed to be small so that an approximation that the cosine term equals one can be done and thus be removed from the equation above. Due to this approximation  $F_{roll}$  becomes constant having only the vehicle mass,  $m$ , and the friction constant,  $c_{roll}$ , as parameter values.

The gravitational force can be expressed as,

$$F_{grav} = mg \sin(\phi) \approx mg\phi. \quad (3.4)$$

As stated above the road gradient is considered to be small, and thus the equation (3.4) can be linearized by substituting the sine term with its argument  $\phi$  [17], making  $F_{grav}$  proportional to the road gradient angle.

The last term in equation (3.1) is the internal friction force,  $F_{fric}$ , arising from rotating parts in engine. The equation for  $F_{fric}$  is given by

$$F_{fric} = \frac{T_{fric}\eta_{wheel}}{r_{wheel}}, \quad (3.5)$$

where  $T_{fric}$  is the friction load torque that counteracts the propelling output torque,  $\eta_{wheel}$  is the efficiency from wheel to engine, i.e. the powertrain, and  $r_{wheel}$  is the radius of the wheel.  $\eta_{wheel}$  and  $r_{wheel}$  is considered to be constant which makes the friction force directly proportional to the friction torque [19].

While driving on a downward slope the  $F_{grav}$  term will change sign due to a change from a positive to a negative road angle, which leads to a gravitational pull and an acceleration of the vehicle. The steeper the road angle is the more the vehicle will be accelerated due to the gravitational force and at a certain angle the gravitational pull will overcome the resistive forces counter acting the movement of the truck. Due to this acceleration braking has to occur in order to keep the set-speed of the vehicle. By using the electric generator to brake the vehicle some of the braking energy can be recuperated. Conventional friction brakes will be used to further slow down the vehicle if the power needed to brake the vehicle to the set-speed exceeds the maximum power of the generator.

## 3.2 Global Simulation Plattform and VSim+

Within Volvo a simulation tool for offline simulations inside Matlab and Simulink is used called the *Global Simulation Plattform* (GSP). GSP contains a model of a truck which consists of different subsystems such as battery packs, ICEs, EMs and several other systems that are present in real trucks. There is also a model of a driver, which is modeled as a PID-regulator and a road environment used to simulate different roads, speeds etcetera. A conventional non-hybrid truck is also included which can be used as a reference tool for benchmarking different results from the hybrid trucks, such as fuel consumption and various performance improvements. The simulation platform was earlier called VSim+ but is now called GSP, even if the name VSim+ is still in use at Volvo.

## 3.3 Drive cycles

When measuring fuel consumption and pollutant emissions from vehicles, standardized *test cycles* may be used. These test cycles are pre-defined cycles with standardized speed- and elevation profiles which makes it possible to compare different vehicles, or vehicle configurations, on the same basis [19]. In the simulation software, such as the GSP platform environment used by Volvo, *road maps* are widely used. These are mappings of different road intervals which contains set-speeds and topography information about the specific road cycles. The data for the maps used in this thesis comes from real routes where an actual truck has gathered the data by using Global Positioning System (GPS), dead reckoning and gyro sensors [24]. The maps are also used to extract future-road data a certain distance ahead of the truck. This is done by choosing all the data from the present position of the truck until the desired position ahead of the truck.

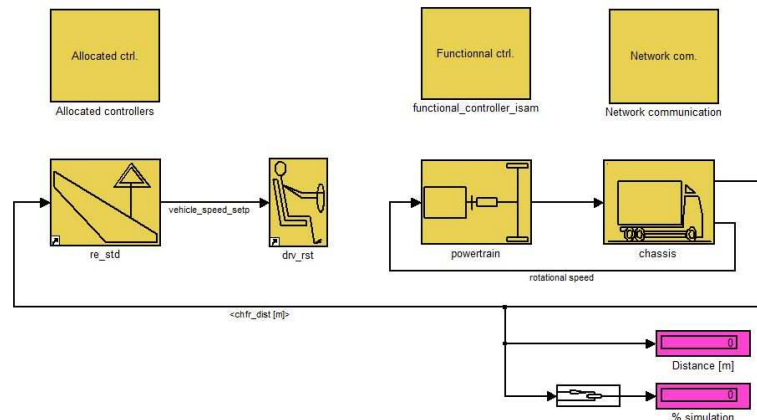


Figure 3.2. The simulation platform. The figure shows the topmost level of the simulation platform, which consists of a truck chassis model, a driver model and the road environment (drive cycle). These models are built up by several subsystems.

Three such drive-cycles were used for simulations and testing of the predictive energy management algorithms. These routes were the ones between Borås-Landvetter-Borås in Sweden, Paris- Lille in France and Frankfurt-Koblenz in Germany. Abbreviations were used in order to shorten the names of the routes, which can be found in figure 3.3.

Full name	Abbreviation
Borås-Landvetter-Borås	BLB
Paris-Lille	PL
Frankfurt-Koblenz	sx135

Figure 3.3. Abbreviations for the three drive-cycles.

The drive-cycles are given as matrices within GSP, where each column is a function of the distance and represents a certain data, e.g. the set-speed. The resolution of the data is segments of about 60 meters for Borås-Landvetter-Borås and Paris-Lille and about 500 meters for the Frankfurt-Koblenz drive-cycle.

The road environment has a big impact on the fuel consumption of the vehicle, where roads with many steep hills lead to higher average fuel consumption. But the road environment also affects the efficiency of the hybrid system. If the drive-cycle contains many steep hills, the speed of the vehicle will increase while rolling down the hills because of the gravitational pull. The vehicle then has to decelerate by using its brakes in order to hold the set-speed and while doing so recuperation may be used. Therefore a hybrid system will be more beneficial on hillier roads, since the percentage in fuel savings compared to a conventional truck will increase. How hilly a certain route is may be defined by the *average road gradient* factor. A

high average road gradient factor states that the route is hilly and a relatively low value states that the route is flat. It has however been shown by Volvo that this correlation between fuel-savings and increasing average road gradient has a limit for a given hybrid system [5]. If the road is too hilly the hybrid system gets saturated and the rest of the energy will therefore disappear as heat in the brakes.

Further information about the drive cycles can be found in Appendix D.

Distance [m]	Speed [m/s]	Altitude [m]
1084.15	23.61	127.87
1140.24	23.61	127.73
1196.34	23.61	127.20
1252.44	23.61	126.76

Figure 3.4. A road-map example. The figure shows a few data points taken from a road map. The columns, read from left to right, give the distance from the starting position, the speed that has to be hold and the altitude of the road in meters above sea level, respectively.

### 3.4 e-Horizon and estimation of future road data

The ADAS RP (Advanced Driver Assistance System Research Platform) developed by Navteq can provide information of upcoming road events when it has access to the position of the vehicle. The position of the vehicle comes from a combination of the three positioning methods described in section 3.3 and an onboard map. The ADAS RP is able to calculate the probability for which routes the driver will drive within a certain distance ahead of the vehicle. The combination of routes that give the highest probability will be used as an electronic preview horizon, the *e-Horizon*. The data for upcoming events within the preview horizon comes from a map-database, similar to the road-maps described earlier. The prediction-based energy management strategies will be based on such data. The distance of the preview horizon will be referred to as the *e-Horizon length* within this thesis.

## 4 The hybrid truck model

This chapter presents the concept of the hybrid technology used for the truck and the key components within that technology. The chapter rounds up with a description of the truck model at a component level and the power flows in the powertrain.

### 4.1 Parallel hybrid

Hybrid vehicles can be classified according to the way they supply power to the powertrain and there are three main types; the series hybrid, the parallel hybrid and the combined hybrid. The truck that was used for simulations is a parallel diesel-electric hybrid. There will be some comparisons made between the series- and the parallel hybrid and the interested reader can find more information about the series hybrid in Appendix E.

In a parallel hybrid the ICE and the EM are both connected to the same drive shaft and can simultaneously transmit power to drive the wheels. Parallel HEVs can be classified according to the degrees of hybridization they belong to, where the two most common types are the mild hybrid vehicle and the full-hybrid vehicle. The mild hybrid (see figure 4.1) vehicle is a vehicle that cannot drive on electricity alone because the power output of the electric propulsion system is too small to propel the vehicle on its own. It is only supposed to contribute with some of the power needed for the propulsion, e.g. for keeping the ICE at some optimal operating point. In this case the ICE can either operate alone on the drive shaft or operate together with the EM, but the electric motor can never operate on its own. The combined power of the ICE and the electric motor will be the propulsive power of the vehicle. A full hybrid vehicle is a vehicle that can run on electricity- or the engine alone, or a combination of these two. A full hybrid vehicle usually requires a large battery pack.

The fact that there are many possibilities on how to combine the power from the ICE and the electric motor adds another *degree of freedom* (DOF) in order to meet the power demands of the vehicle [40]. The control of the power split between the different propulsion systems within an HEV is often referred to as *supervisory control* or *energy-management*. There are mainly two different ways to control an HEV. One is *heuristic- or rule based control* in which every action is predefined, but there are also more dynamic types of control [40].

The advantage of a parallel hybrid over a series hybrid system is that the parallel hybrid only needs two machines, one engine and one EM. The disadvantage is that a clutch is needed because the engine is linked to the powertrain. Nevertheless, the mild hybrid system will also have recuperative abilities so that some of the energies that otherwise would be lost during driving can be recuperated.

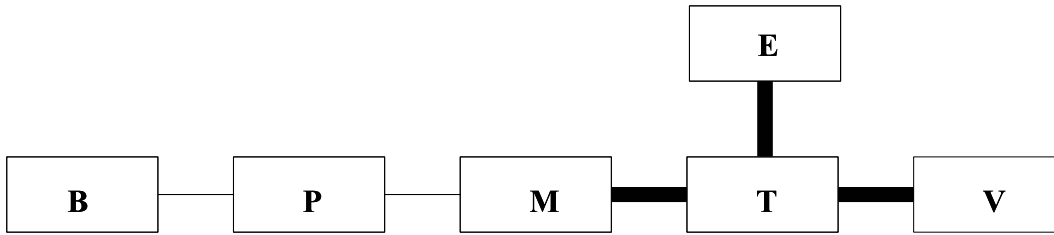


Figure 4.1. Full parallel hybrid configuration. B: battery, E: engine, M: motor, P: power converter, T: transmission (including clutch and gears), V: axles and vehicle. Bold lines: mechanical link, solid lines: electrical link.



Figure 4.2. Mild parallel hybrid configuration. B: battery, E: engine, M: motor, P: power converter, T: transmission (including clutch and gears), V: axles and vehicle. Bold lines: mechanical link, solid lines: electrical link.

## 4.2 Electric storage system

The electric storage system (ESS) is usually a Li-ion or NiMH based battery or a super capacitor. These electric storage devices are bi-directional which means that they can be charged and discharged while the vehicle is driving [28]. Even the most advanced batteries available at present time can only store a fraction of the energy per unit weight compared to gasoline, as can be seen in figure 4.3. Therefore it is yet not possible to have the same performance on vehicles running on a pure electric propulsion. In the sequel the battery together with its converter will be declared as *ESS*.

An important factor of the battery is the *state of charge* (SoC) which states the current charge of the battery. If SoC is 100 percent the battery is fully charged and if it is zero percent then the battery is completely discharged. The lifetime of a battery is closely connected to the *depth of discharge* (DoD) and it is generally not good to fully deplete or fully recharge a battery since this will decrease the battery lifetime [19]. To enhance the lifetime of a battery only a fraction of its full capacity is therefore used. This fraction, or interval, is called the *State of Charge window* (SoC-window) and is bounded by an upper and lower SoC limit. In figure 4.4 this window has been highlighted between 30- and 60 percent SoC-value, since that is the SoC-window in use by Volvo and that will also be used within this thesis. What decides the size on the SoC-window depends heavily on the battery and its application. Figure 4.4 shows the SoC value on the y-axis as a percent of battery charge.

The state variable, SoC, cannot be directly measured but can instead be estimated based on the energy flow within the battery, if the initial condition is known [19]. When recuperating, a formula for the SoC-change based on the ratio between the

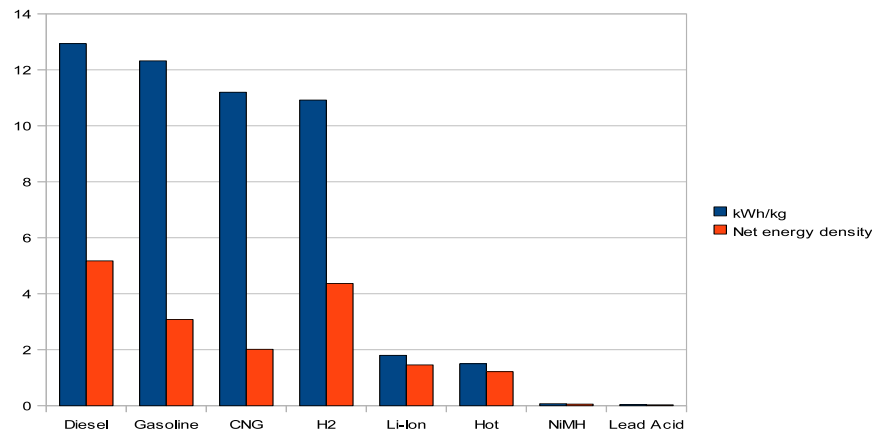


Figure 4.3. Energy density of different on-board energy storage sources. The blue bars indicate the actual chemical energy available and the orange bars represent the energy that will be available at the wheels when energy losses from the combustion and the powertrain are considered.

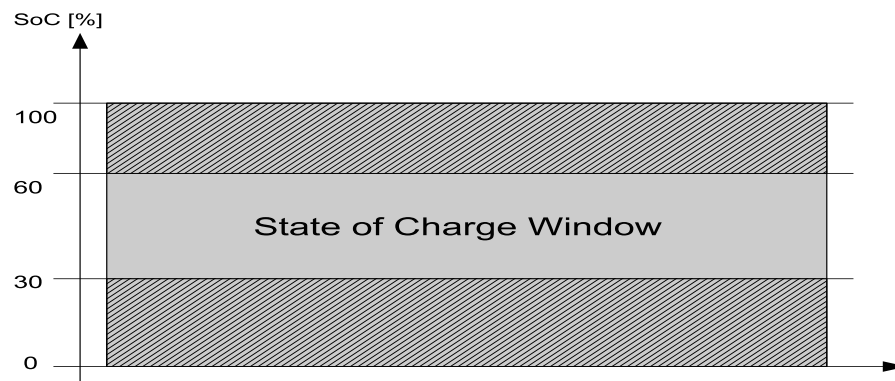


Figure 4.4. Illustration of the state of charge and the definition of state of charge window.

recuperation energy and the nominal battery charge level can be derived as [3]

$$\Delta SoC = \frac{E_{recup}}{E_{nom}}. \quad (4.1)$$

## 4.3 Internal Combustion Engine

The internal combustion engine (ICE) in the truck is a 460 horsepower Volvo diesel engine with a maximum output torque of 2700 [Nm]. This is the main power unit in the powertrain, converting chemical energy from a fuel/air mixture into mechanical power in the driveline. Inside of GSP the ICE is approximated by *motor maps*. This approximation, or model, is a two-dimensional matrix that specifies the fuel-

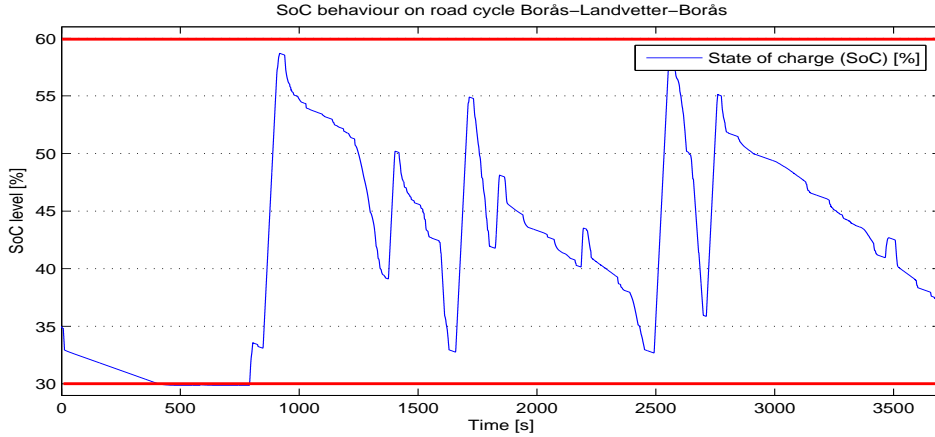


Figure 4.5. SoC-level example for the BLB drive-cycle. This is an illustration of how the SoC changes within the ESS throughout the drive-cycle. These kind of plots give a good overview of how the energy within the ESS is used and will be used in the sequel of this paper to compare and analyze results from the different energy management strategies.

mass flow,  $\hat{m}_f$  [ $kg h^{-1}$ ], as a function of the operating points, which are defined by the engine speed,  $\omega$  [rad/s], and the engine torque,  $T_{ICE}$  [Nm] (see figure 4.6). The data in the motor-map is gathered by measuring the corresponding outputs for certain inputs (operating points) in test benches. All outputs are measured at steady-state conditions. The resolution of the measured points can be increased by linear interpolation.

Engine speed [rad/s] →	$\omega_1$	$\omega_2$	$\omega_3$	...
Torque output [Nm] ↓				
$T_1$	$m\hat{f}_{11}$	$m\hat{f}_{12}$	...	
$T_2$	$m\hat{f}_{21}$			
$T_3$	⋮			
⋮				

Figure 4.6. An ICE motor-map example from GSP. The left-most column and the upper-most row together define the desired operating point, declaring the demanded output-torque,  $T$ , and engine speed,  $\omega$ , respectively. The output is given as the fuel-mass flow rate,  $\hat{m}_f$ .

The produced chemical power for a certain operating point can be found by using the following formula:

$$P_f(t, u(t)) = H_{LHV} \cdot \hat{m}_f(t, u(t)), \quad (4.2)$$

where  $P_f(t, u(t)) = H_{LHV} \cdot \hat{m}_f(t, u(t))$  is the fuel power input to the ICE with  $H_{LHV}$

[J/mg] being the lower heating value of the fuel. The variable  $u(t)$  is the control signal.

## 4.4 Electric motor

The electric motor (EM) is the secondary power source in the powertrain of the truck. The EM produces mechanical power by converting electric energy from the ESS, leading to a discharge of the battery. When the vehicle is braking the EM acts as a generator and recharges the battery by recuperation. The EM is modeled with motor-maps, similarly to the ones used for the ICE, but instead of having the fuel-mass flow as output, the efficiency values of the EM are given at each operating point (see figure 4.7).

Engine speed [rad/s] →	$\omega_1$	$\omega_2$	$\omega_3$	...
Torque output [Nm] ↓				
$T_1$	$\eta_{11}^{EM}$	$\eta_{12}^{EM}$	...	
$T_2$	$\eta_{21}^{EM}$			
$T_3$	⋮			
⋮				

Figure 4.7. An EM motor-map example. The left-most column and the upper-most row together define the desired operating point, declaring the demanded output-torque,  $T$ , and engine speed,  $\omega$ , respectively. The output is given as the efficiency of the EM,  $\eta^{EM}$ , at that operating point.

## 4.5 Engine Electronic Control Unit

The powertrain is controlled by different Electric Control Units (ECU's) and they all use the CAN-bus to communicate. The Engine Electronic Control Unit (EECU) controls the operation of the engine as well as how the torque distribution in the powertrain is split between the EM and the ICE.

## 4.6 The truck model

The truck is a diesel-electric driven mild parallel hybrid truck. Two ESS-packages of different capacities and two EMs with different power-outputs were chosen from within GSP to model different hybrid systems in the truck. Combining the ESS-packages and EMs gave four different hybrid set-ups. Figure 4.8 gives the data for the EMs and ESS that were used and it also gives the mass of the truck. Figure 4.9 shows the schematic over the important systems within the truck model. The schematic consists of the electric storage system (ESS)- which in this case is a

Total mass [kg]	40000
Electric motor <sub>1</sub> [kW]	60
Electric motor <sub>2</sub> [kW]	120
Battery <sub>1</sub> [kWh]	0,6
Battery <sub>2</sub> [kWh]	1,35

Figure 4.8. Different parameters that were used in simulations of the truck. The mass was hold constant.

battery, the EM, the ICE, the clutch, the mechanical auxiliaries (MAUX) and the electric auxiliaries (EAUX) of the long haul truck. The electric- and mechanical auxiliaries are external systems that drain a constant of 1,1 [kW] of electric energy and 2 [kW] mechanical energy. The energy for the EAUX is fed from the ESS as long as it is not depleted.

The EM is mounted directly on the driveshaft between the clutch and the gearbox and can be used for both propulsion and as a generator, eliminating the need for a separate generator. It is possible to feed the EM directly from the ICE and thus use it as a fuel-driven generator in order to charge the battery. Doing so the efficiency will approximately be  $\eta_{FuelCharge} = \eta_{ICE} \cdot \eta_{EM} \cdot \eta_{ESS}$  which is an under average efficiency and will lead to high energy losses, therefore this function is never used in normal conditions. Nevertheless the ICE will start to feed the generator in order to produce electric power if the battery has reached the lower boundary of the SoC-window and recuperation (braking) is not occurring. This is done in order to deliver the needed energy for the EAUX within the truck and it is a build-in algorithm within GSP.

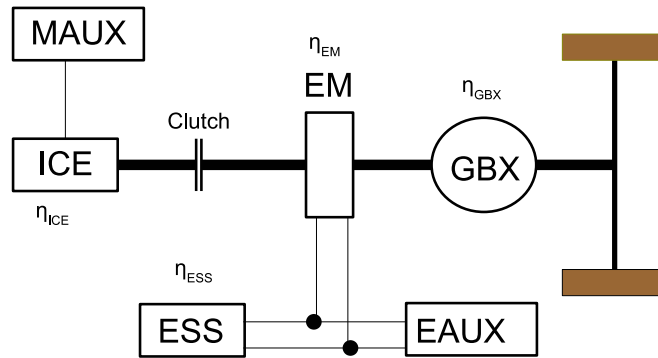


Figure 4.9. Schematic of the truck model.

The ICE and EM are modeled just by the motor-maps that were introduced in sections 4.3-4.4. The gearbox was not included in the model. This simplification would not affect the results significantly while the gear is mostly hold constant and shifted very seldom for the long haul trucks used within the simulations. However there were some efficiency losses,  $\eta_{GBX}$ , in the gearbox which were included in the calculations.

## 4.7 Torque distribution

The performance of a hybrid system depends heavily on how the energy is distributed between the ICE and EM. In some situations it may be favorable to take all the power from the ICE and none from the EM, for example when the ESS is low on SoC. Doing so would mean that the truck is operated as a conventional vehicle. On the other hand if the ESS is high in SoC it may be favorable to use the EM as much as possible and the ICE as little as possible in order to save fuel and lower the emissions. The laws of how the energy-flow from the ICE and the EM are controlled will be called *energy management strategies* in the sequel. Within GSP the energy-flow at the powertrain is controlled by how the torque is split between the ICE and the EM. In case of the real Volvo truck and the model within GSP, this function is software-based and located in the EECU. As stated in the beginning of this paper the objective is to find prediction based energy management strategies with an aim at lowering the fuel consumption.

At every given time there will be a *torque demand*,  $T_{DEM}$ , at the wheels of the vehicle which has to be met in order to hold the set-speed of the truck. This demand depends on the set-speed itself, the mass of the truck, the external forces acting on the vehicle and the topology of the road. How these external forces and road topology are affecting the vehicle can be calculated with the equations given in section 3.1. While both the ICE and the EM are acting on the same driveshaft, their combined power has to fulfill  $T_{DEM}$ <sup>1</sup>, that is

$$T_{DEM} = T_{ICE} + T_{EM}, \quad (4.3)$$

By rewriting 4.3 into a power-term it is possible to make a power-flow description of the powertrain,

$$P_{Tot} = P_f(t, u(t)) \cdot \eta_{ICE} - P_{MAUX} + P_{ESS}(t, SoC, u(t)) \cdot \eta_{EM} - P_{EAUX}, \quad (4.4)$$

where  $P_{ESS}(t, SoC, u(t)) = U \cdot I(t, u(t))$  is the power-output from the ESS being a function of the voltage,  $U$ , and current,  $I(t, u(t))$ , output.  $P_{EAUX}$  is a constant power-supply to the electric auxiliaries and  $P_{MAUX}$  is a constant power-supply to the mechanical auxiliaries. The control variable  $u(t)$  is in this case chosen to be the torque-output from the EM,  $T_{EM}$ . The parameters  $\eta_{ICE}$ ,  $\eta_{EM}$  and  $\eta_{ESS}$  are the efficiency values for the ICE, the EM and the ESS respectively.

The ESS is one of the most advanced models within GSP and the efficiency value,  $\eta_{ESS}$ , is not constant but depends mostly on the power input- and output of the

---

<sup>1</sup>If this constraint cannot be fulfilled, for example due to a  $T_{DEM}$  which is higher than the torque that the ICE and the EM can deliver, it will cause a speed-decrease of the vehicle and the set-speed cannot be hold.

battery<sup>2</sup>. By making a least-squares approximation of the power-losses from the ESS as a function of the current-flow a mathematical expression was obtained for  $\eta_{ESS}$ . While the torque-output from the EM,  $T_{EM}$ , is the control signal and can be chosen freely<sup>3</sup>, and the torque-demand at the wheels,  $T_{DEM}$  is given at every time-step, only the torque-output from the ICE has to be calculated. This can be done by rewriting equation (4.3) into:

$$T_{ICE} = T_{DEM} - T_{EM}. \quad (4.5)$$

---

<sup>2</sup>The efficiency,  $\eta_{ESS}$ , also changes depending on if the ESS is being charged or de-charged.

<sup>3</sup>As long as it is kept within the fulfills the maximum and minimum torque outputs from the EM.

# 5 Optimization

Optimization is the act of choosing the *best possible solution* for a given problem where usually one or several constraints have to be satisfied as well. The optimization method used for the energy management strategies within this thesis are based on optimal control theory, which will be explained next.

## 5.1 Optimal control

The optimal control problem deals with one or more control laws that tries to optimize (minimize or maximize) a certain criteria called the *cost function*<sup>1</sup> while at the same time satisfying some physical constraints [32]. The cost function is a function of the states for the plant. When one talks about optimal control it is usually a set of differential functions describing the paths of the control variables that minimize the cost function [48].

A general performance index including various minimization or maximization elements, such as pollutant emissions or drivability measures<sup>2</sup> [19], has the following form

$$J = \int_{t_0}^{t_f} P_f dt = \int_{t_0}^{t_f} L(t, x(t), u(t)) dt, \quad (5.1)$$

where  $L(t, x(t), u(t))$  is the cost function which includes all the elements that need to be optimized,  $t$  stands for time,  $x(t)$  is the state variable and  $u(t)$  is the continuous control signal.

The objective of this thesis work is to find energy management strategies that optimize the torque-split between the internal combustion engine and the electric motor in such a way that the fuel consumption is minimized. The main task of these strategies is not to minimize the fuel mass-flow rate at each instant of time, but rather to minimize the *total* fuel-consumption along a given route. The energy management system can be formulated as a convex constrained optimization problem over the route, having the  $T_{EM}$  as control signal,  $u(t)$ . If the torque and speed requests trajectory at the powertrain are perfectly known over a time interval  $[t_0, t_f]$  of the route, a deterministic energy management problem can be derived [23],

$$J = \int_{t_0}^{t_f} H_{LHV} \cdot \hat{m}_f(t, SoC, u(t)) dt. \quad (5.2)$$

---

<sup>1</sup>Cost functions can also be referred to as *performance indexes* in the literature.

<sup>2</sup>How crucial these elements are for the optimal solution may be defined by introducing weighting factors for each elements.

where  $u(t)$  is the control signal which is calculated from the present torque and speed requests at the powertrain and is subject to constraints due to the limitations of the hybrid system components.

Within a hybrid electric vehicle the solution for (5.2) would be to only use electric energy, while such a solution gives a minimum amount of fuel mass consumption. A pure electric drive is possible if three criteria are fulfilled

1. The battery capacity is large enough to deliver energy during the whole driving cycle.
2. The regenerative energy that is available during the cycle is enough to ensure that the battery is not completely discharged until the end of the mission.
3. The electric drive system is powerful enough to ensure that the demanded power during the cycle will always be met.

As mentioned in section 4.2 even the most powerful batteries available at present time are still ineffective in storing energy per unit weight compared to the energy content of fossil based fuels and a pure electric drive would not fulfill the duty cycle of a long haul truck. To prohibit pure electric solutions equation (5.2) is subject to the following final battery level and component constraints:

$$\frac{dSoC}{dt} = f(t, SoC, u(t)), \quad (5.3)$$

$$SoC(t_f) = SoC(t_0), \quad (5.4)$$

$$SoC_{min} \leq SoC(t) \leq SoC_{max}, \quad (5.5)$$

$$u(t) \in \Gamma. \quad (5.6)$$

Constraint (5.5) puts a requirement on the system that the final charge has to be the same as the initial charge. Equation (5.6) requires the control signal  $u(t)$  to be in an admissible set of control inputs. In (5.2) SoC is defined as

$$\dot{SoC} = -\eta_{ESS} \cdot P_{ESS}, \quad (5.7)$$

where  $P_{ESS}$  is the power output from the ESS,  $\eta_{ESS}$  being the efficiency of the ESS. Equation (5.7) is subject to the following two cases:

- discharge;  $P_{ESS} > 0, \eta_{ESS} > 1$
- charge;  $P_{ESS} < 0, \eta_{ESS} < 1$ .

The constraints (5.4-5.6) prohibit the solution of (5.2) to be pure electric.

## 5.2 Equivalent Consumption Minimization Strategy

The equivalent consumption minimization strategy (ECMS) has been shown to be an effective method of making optimal energy management strategies in the causal case when preview information is not available [13, 16]. The ECMS approach introduces an *equivalence factor*,  $s(t)$ , into the cost function (5.2), which transforms electric energy into equivalent fuel energy [4, 37]. This equivalence factor is the core of the ECMS algorithm [14]. The ECMS approach is also called a *cost-based strategy*, *real-time control strategy*, or *online optimization strategy* [19].

By using the maximum principle [15, 43, 38, 29] the following Hamiltonian can be derived that gives the optimal path along the solution for (5.2):

$$H(\text{SoC}(t), u(t), s(t), t) = P_f - s \cdot P_{ESS} \cdot \eta_{ESS}, \quad (5.8)$$

with

$$P_{ESS} = \frac{P_{EM}}{\eta_{EM}}, \quad (5.9)$$

where  $\eta_{ICE}$ ,  $\eta_{EM}$  and  $\eta_{ESS}$  are the efficiencies for the ICE, the EM and the ESS respectively.  $P_f$  is the fuel power given in (4.2) and  $P_{EM}$  is the power output from the EM. Equation is subject to the following two cases:

- traction;  $\eta_{EM} < 1, P_{ESS} > 0$
- charge;  $\eta_{EM} > 1, P_{ESS} < 0$ .

The equivalence factor,  $s(t)$ , which corresponds to the adjoint state in classical optimization theory [40, 19], is described by the Euler-Lagrange equation

$$\dot{s} = -\frac{\partial H(\text{SoC}(t), u(t), s(t), t)}{\partial \text{SoC}}. \quad (5.10)$$

In the ECMS algorithm an approximation is made that the dependency on the SoC can be disregarded. This approximation holds since only larger deviations of the SoC may cause variations on the internal battery parameters. The approximation is however not valid for e.g. hydraulic hybrids [11] or HEVs with super capacitors [15, 23]. With the SoC dependency disregarded the adjoint state will be approximately constant along the optimal path [40, 23], that is

$$\dot{s} = -\frac{\partial H(u(t), s(t), t)}{\partial \text{SoC}} \approx 0. \quad (5.11)$$

The optimal control signal<sup>3</sup>,  $u^*(t)$  is then found by minimizing equation (5.8)

$$u^*(t) = \arg \min_{u(t)} \left\{ \frac{P_{ICE}}{\eta_{ICE}} - s \cdot P_{EM} \cdot \frac{\eta_{ESS}}{\eta_{EM}} \right\}. \quad (5.12)$$

This equation is subject to the following constraints

$$T_{ICE} + T_{EM} = T_{DEM}, \quad (5.13)$$

$$T_{ICE,min} \leq T_{ICE} \leq T_{ICE,max}, \quad (5.14)$$

$$T_{EM,min} \leq T_{EM} \leq T_{EM,max}. \quad (5.15)$$

The ECMS approach requires a good model for the power-flow in the powertrain. The equations given in section 3.1 and 4.7 were used for modeling the powertrain and the demanded power from the various components.

The equivalence factor  $s$  can be seen as a trade off or as a cost off using electric energy relative to using chemical energy stored in fossil fuels [3]. This implies that a low value of the equivalence factor will make the cost of using electric energy low relative to using chemical energy and the solution of (5.12) would be to demand more torque from the electric motor and less from the internal combustion engine. If the value of the equivalence factor is high the solution would tend to demand less torque from the electric motor and more from the internal combustion engine. There exists a certain threshold value for the equivalence factor after which torque is being demanded also from the ICE as a solution for (5.12). This value is approximately

$$s_{balance} = \frac{\eta_{EM}}{\eta_{ICE}}, \quad (5.16)$$

where  $\eta_{EM}$  is the efficiency of the electric motor and  $\eta_{ICE}$  is the efficiency of the internal combustion engine.

As long as the value of the equivalence factor is below the value given by (5.16) the solution of (5.12) would be to always use as much torque as possible from the EM and the rest from the ICE in order to fulfill (5.13). When the equivalence factor reaches this certain balance value the torque demand from the EM will decrease as the equivalence factor increases. When the equivalence factor reaches a high-enough value the solution of (5.12) will instead be to demand maximum torque output from the ICE and no torque from the EM.

---

<sup>3</sup>Since the approximation has been made that the adjoint state is constant, the optimal solution can be found by the minimization of a function instead of an integral.

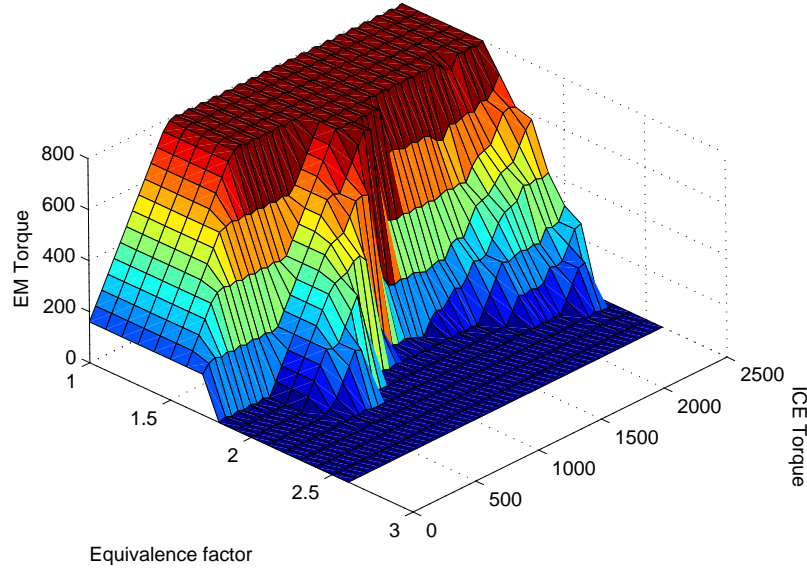


Figure 5.1. Graphical view of the ECMS look-up table. The graph shows the optimal EM torques,  $\tilde{T}_{EM}$ , for a range of torque demands,  $T_{DEM}$ , and equivalence factors. The engine speed,  $\omega$ , is in this case 1200 rpm.

All solutions for (5.12) can be computed off-line for a combination of all the allowed values for the operating points ( $T_{DEM}$  and engine speed) and the range of equivalence factors that have been chosen. The solutions can then be stored in a three-dimensional look-up table to reduce on-line calculation time. The inputs of the table are  $T_{DEM}$ ,  $\omega$ ,  $s$  and the output is  $\tilde{T}_{EM}$ , the optimal torque output from the EM for a given demanded operating point (see figure 5.1). The equivalence factor can therefore be used to control the usage of the EM and also the torque-split within the hybrid powertrain.

The question then arises of how to choose the best possible equivalence factor,  $s$ . Since the objective of this thesis is to reduce the fuel consumption of the vehicle the equivalence factor should be chosen in such a way that the overall fuel consumption on a route is lowered. Chapter 6 will describe how the equivalence factor is calculated in the present, non-predictive, energy management strategy used by Volvo. Chapter 7 will present the prediction based methods to calculate the equivalence factor that were developed within this thesis.

## 6 The non-predictive energy management strategy

The present energy management strategy in use by Volvo is non-predictive and does not use any information about future road environments. In this strategy the equivalence factor,  $s$ , that was introduced in section 5.2 is purely based on the present SoC-level within the ESS. This strategy will be used as a reference for how well the predictive energy management strategies given in chapter 7 performed. This chapter will introduce the functionality of this non-predictive method to calculate the equivalence factor, and the main parameters describing it will be given.

### 6.1 Non-predictive equivalence factor

The present energy management strategy uses a set of predefined values for the equivalence factor for every possible SoC-value. The idea is that the equivalence factor is high when the SoC-level in the ESS is very low, leading to an energy usage that is costly relative to fuel energy. And if the SoC-level within the ESS is very high the equivalence factor is set to a low value making the use of electric energy "cheap" relatively to fuel energy so that the EM is used more in order to assist the ICE. Between these two borders the weight factor is set to the balancing value given by equation (5.16). An example of this function can be found in Figure 6.1.

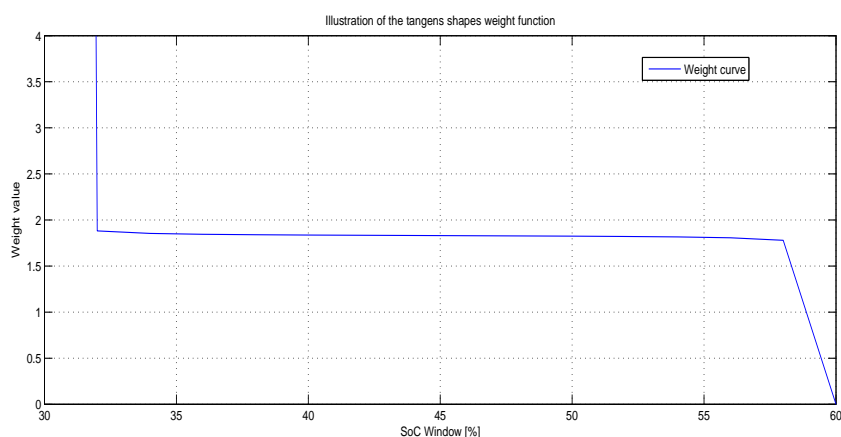


Figure 6.1. Illustration of the equivalence factor function. The SoC-window is on the x-axis while the equivalence values are presented on the y-axis.

Since the equivalence factor is set to the balancing value (5.16), which is a relatively low value, throughout most of the SoC-window the EM will be used frequently which leads to a fast depletion of the electric energy within the ESS. This phenomenon can be seen in Figure 6.2 which shows the resulting SoC-curve when using the non-

predictive strategy for the BLB drive cycle. In this picture it is clear that the energy within the ESS (the SoC-value) decreases very fast. This strategy is effective in the non-predictive case since there is no knowledge of when the next recuperation phase may occur. Therefore the energy is used up as fast as possible in order to make room for possible upcoming recuperation. The disadvantage of such a strategy is that the electric energy is not preserved and used when it is most optimal, for example from a fuel saving perspective. It will also lead to frequent saturations at the lower boundary of the SoC-window and the ICE will therefore feed the generator in order to feed the EAUX, as explained in section 4.6.

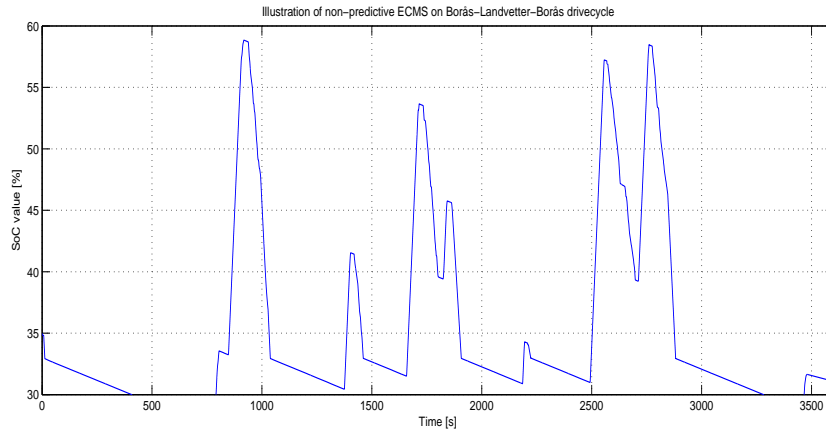


Figure 6.2. SoC-curve for the BLB drive cycle using the non-predictive energy management system. The strategy is to deplete the ESS from energy as fast as possible to avoid an under-used hybrid system.

The values for the equivalence function from Figure 6.1 are defined by a set of functions, these are

$$Rt_a = -\frac{\pi}{Rt_{SoC,upper} - Rt_{SoC,lower}} \quad (6.1)$$

$$Rt_b = \frac{\pi}{2 - Rt_a \cdot Rt_{SoC,lower}} \quad (6.2)$$

$$Rt_k = -\frac{Kp_{SOCCref} \cdot \cos(Rt_a \cdot Rt_{SOCCref} + Rt_b)^2}{Rt_a} \quad (6.3)$$

$$Rt_m = Rt_{WeightRef} - Rt_k \cdot \tan(Rt_a \cdot Rt_{SOCCref} + Rt_b) \quad (6.4)$$

where  $Rt_a$  determines the width of the function to match the SoC window (30% – 60%),  $Rt_b$  determines where on the SoC-window (x-axis) the center of the equivalence factor function should be positioned,  $Rt_k$  decides the horizontal angle of the function and  $Rt_m$  determines its vertical position. The interesting parameters in equations (6.1) - (6.4) above are,  $Rt_{SOCCref}$ ,  $Kp_{SOCCref}$  and  $Rt_{WeightRef}$ . A short description for these parameters is given in the list below:

- $Rt_{SOCCref}$  decides the longitudinal position<sup>1</sup>.

<sup>1</sup>Absolute center will be established between a value of 0 to 100.

- $Kp_{SOCRef}$  decides the slope of the curve near  $min$  and  $max$  of the SoC window.
- $Rt_{WeightRef}$  decides the balance value mentioned above.

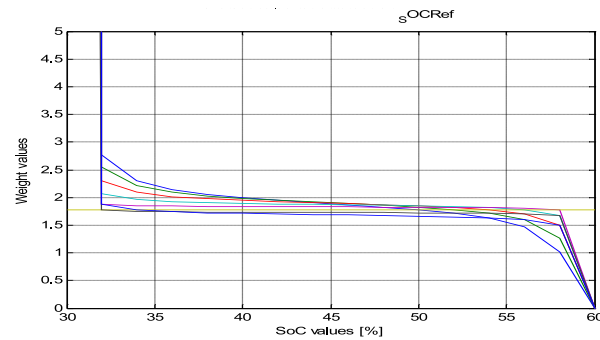


Figure 6.3. Illustration for the effect of manipulating the  $Rt_{SOCRef}$  parameter. Changing this parameter will make the transition between the balance value and the end values smoother.

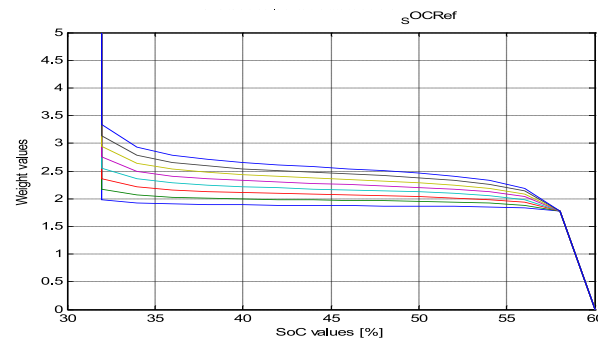


Figure 6.4. Illustrates the effect of manipulating the  $Kp_{SOCRef}$  parameter. It is seen that the gradient of the balance value is changed when altering this parameter.

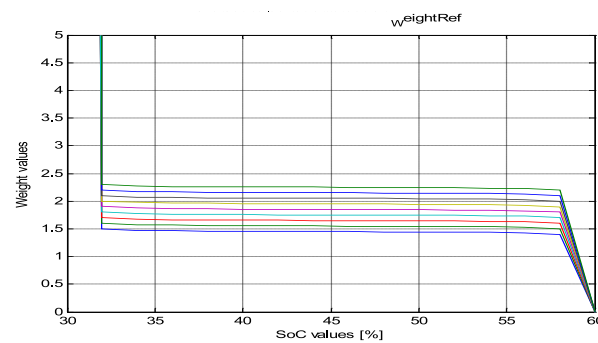


Figure 6.5. Illustrates the effect of manipulating the  $Rt_{WeightRef}$  parameter. This decides the level of the balance value and simulations shows that it has a more substantial effect on the fuel consumption than the other two parameters

---

In Figures 6.3 - 6.5 examples are illustrated of how the equivalence factor function is changed when altering the different parameters. These parameters can be tuned in for optimal performance in different hybrid set-ups and drive-cycles. Having so many parameters leads to many simulations to be run before a good solution is found. That may be possible to do in a simulation environment but in reality it is not feasible. The tuned parameters will also be highly dependent on the actual truck with its hybrid set-up and the drive-cycle, making this strategy less robust. This makes this non-predictive weight function a far from optimal way of implementing the ECMS. In the next chapter a predictive approach to this problem will be made that is shown to be a better solution to the ECMS problem.

# 7 Predictive energy management

This chapter will present the predictive energy management strategies that were outlined within this master-thesis. Given that future road data is known, such as the topography of the road and the set-speed ahead of the vehicle, the forces that will be affecting the truck and the power that has to be delivered to the wheels of the truck in order to hold the set-speed ahead can be calculated in advance by the equations given in section 3.1. That leads to new opportunities on how to decide the equivalence factor in an optimal manner to further improve the control of the torque-split between the ICE and EM. As explained in chapter 1 the improvement of the torque-split is done in two steps. The first step is to deploy the ECMS-strategy outlined in section 5.2 which minimizes efficiency losses of the ICE and the EM, and the second step is by improving the usage of the ESS so that saturations of it are avoided<sup>1</sup>.

It is most critical to prohibit saturations at the upper boundary of the SoC-window, since that leads to a maximum charged battery which then inhibits further recuperation. By using prediction it is possible to detect such problems in advance and the equivalence factor (5.11) can be controlled so that the electric energy flow is controlled to avoid such saturations, for example by using up enough of electric energy from the ESS just before recuperation takes place so that there will be sufficient re-chargeable capacity left in the ESS. The problem of reaching the lower boundary of the SoC-window is not as grave while there will still be much capacity left for further recuperation inside the battery. The disadvantage of being at the lower side of the boundary, which is the same as having an energy-depleted battery, is that there will not be any energy left to feed the EAUX of the vehicle. If there is not a recuperation-phase at the same time, or just after, as the battery is depleted the energy for the EAUX will be taken from chemical fuel. The ICE will then be feeding the EM in reverse, and take the role of a generator, in order to deliver electric energy to the EAUX, as explained in section 4.6. This operation has to be avoided as much as possible since it will lead to high efficiency losses.

## 7.1 Introductory theory

This section gives the theory of how to predict future forces that will be acting on the vehicle. These predictions will then be used by all the prediction-based energy management systems to calculate how much energy that is available within the e-Horizon.

---

<sup>1</sup>Both the predictive and non-predictive strategies use the ECMS-strategy to minimize the combined efficiency losses between the ICE, the EM and the ESS. Therefore most of the benefits of using predictive strategies over non-predictive strategies will come from an improvement of the ESS usage.

### 7.1.1 Predicted recuperation

Using the equations derived in section 3.1 and the preview data for the road topography the forces acting on the vehicle while at a downward slope can be predicted. When the vehicle reaches a downward slope it will start accelerating due to the gravitational pull. It is assumed that the cruise control is activated which will make the vehicle start braking in order to hold the set-speed. The brake force that can be recuperated into the ESS can then be formulated as

$$F_{i,lim} = \max \left\{ F_i, \frac{P_{GENmax}}{\bar{v}_i \eta_{recup}} \right\}, \quad (7.1)$$

where  $i$  represents the  $i$ :th recuperation interval,  $F_{i,lim}$  is the limited recuperation force due to physical limitations in the hybrid system components.  $F_i$  is the unlimited force acting at the vehicle,  $P_{GENmax}$  is the maximum power input for the generator (maximum recuperable power),  $v_i$  is the vehicle speed and  $\eta_{recup}$  is the efficiency from the wheels to the ESS (including the power-losses within the ESS itself). Saturations within the hybrid system mainly depends on the vehicle speed, the length of the slope, the angle of the slope and on the vehicle mass since these factors affect the braking force.

The recuperable energy is derived as [3]

$$E_{i,recup} = F_{i,lim} \cdot \Delta s \cdot \eta_{recup}, \quad (7.2)$$

where  $\Delta s$  is the recuperation distance (length of the downslope) at which the force affects the vehicle.

### 7.1.2 Overspeed

It is assumed that the driver has the cruise control activated, which is trying to keep the set-speed for the vehicle. When the vehicle starts accelerating in a downward slope due to the gravitational pull the cruise control does however not start braking the vehicle until a certain upper speed-limit above the set-speed has been met. The value at which the actual speed can differ from the set-speed before the cruise control starts braking is called the *over-speed* and is usually 5 [km/h], see Figure 7.1.

This has to be considered in the calculation of the recuperation energy since the recuperation takes place first when the braking speed has been reached and the brakes become active. Since the cruise control does not start braking instantly when the vehicle starts accelerating energy that could be recuperated goes lost, and this energy loss is quite substantial. To predict the over-speed it is assumed that the acceleration is constant over a road interval. This assumption is based on the fact

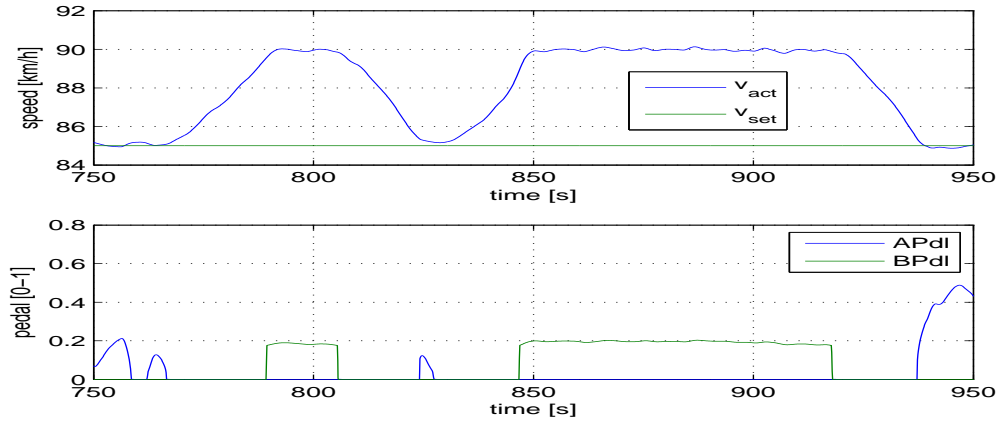


Figure 7.1. Over-speed example. The set-speed (lower line, upper graph) is constant on 85 km/h while the actual speed goes up to 90 km/h. Braking (lower graph, green line) does not occur until the actual speed has reached the set-speed plus the over-speed value at 90 km/h.

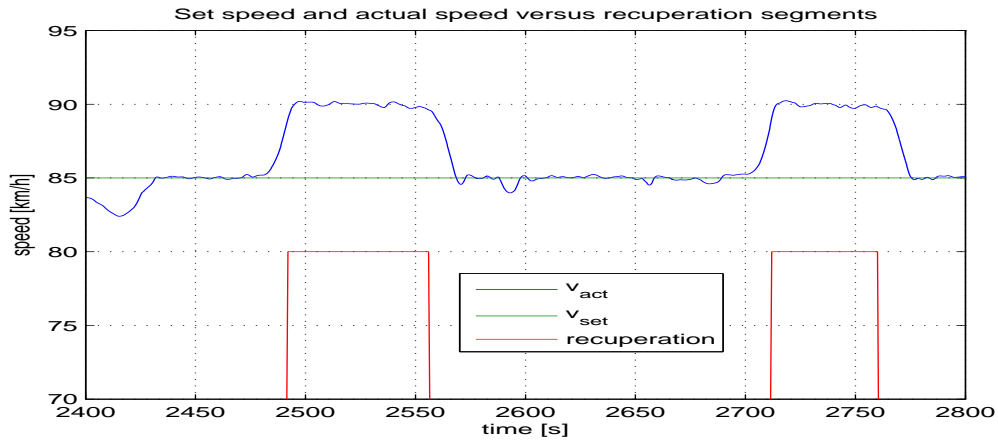


Figure 7.2. Illustrates for the effects of over-speed versus recuperation. It is seen that recuperation is not happening (red line) unless the actual speed has reached 90 [km/h].

that the rate at which the slope changes is considered to be very small. Equation (7.3) below shows the updated speed as a function of present speed and the distance traveled.

$$v = \sqrt{a \cdot \Delta s + v_0^2}, \quad (7.3)$$

where  $a$  is the vehicle acceleration,  $\Delta s$  is the length of the road interval and  $v_0$  is the delivery speed at the beginning of the downward slope. Based on the assumption

that the road gradient is held constant during the road interval  $\Delta s$  one can calculate the speed at the end of each interval using equation (7.3). This knowledge is used to delay the actual recuperation until the speed plus the over-speed has been reached so that the starting point of the recuperation phase is more correct.

## 7.2 Predictive Reference Signal Generator

One of the prediction based energy management strategies that were outlined within this thesis is the *Predictive Reference Signal Generator* (pRSG). This chapter will present the theory of that strategy and conclude with some results.

### 7.2.1 Introduction to the pRSG strategy

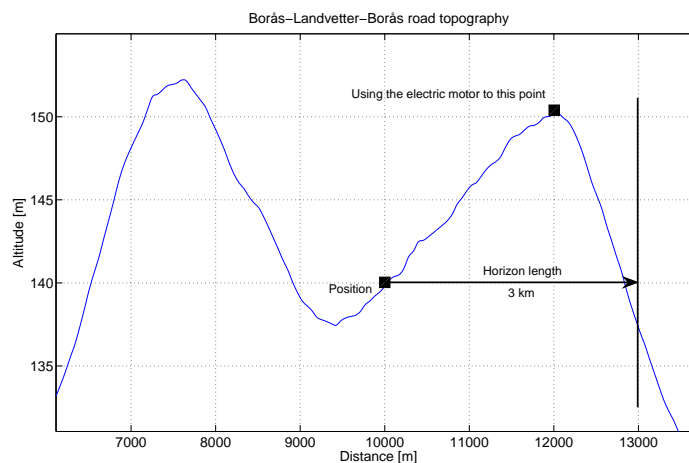


Figure 7.3. Illustration of the idea behind knowledge of future information about the road topography. In figure the position point is the truck current position and the longitudinal line is the end of the e-horizon interval.

The main idea with the pRSG strategy is to construct a reference trajectory for the SoC-value throughout the e-Horizon. This reference should then be the optimal path for using the energy within the ESS having the SoC-window borders as constraints. The reference trajectory tends to discharge the ESS at the slowest possible rate, while still making room for the upcoming recuperation energy within the e-Horizon. This is done by making a SoC-trajectory that discharges the ESS with the same amount of energy that will be recuperated in the next recuperation phase. This requires that the position at the upcoming top of a hill, that is, the point after which recuperation soon will start occurring, is known, which is illustrated in Figure 7.3. By knowing the point on top of the hill the electric motor can then be used optimally, consuming only so much energy that can be recuperated until the end of the e-horizon (longitudinal line). If this information do not exist it will most

likely result in a poor energy management since the battery can be half-full or even completely charged when the top point is reached and thus result in energy losses.

The SoC-reference trajectory is based on the following criteria [3]:

- The signal has to be kept inside the interval  $SoC_{min} \leq SoC \leq SoC_{max}$  (see Figure 7.4)
- The rate of change should be minimized with an appropriate optimization algorithm.

A P-controller is then used to make the actual SoC follow the reference trajectory.

## 7.3 Constructing the Reference Trajectory

This section will explain how the reference trajectory was calculated and introduce the optimization algorithm that was used.

### 7.3.1 Segments

To begin constructing the reference signal for the e-Horizon, the data will be divided into ordered segments. These segments will be labeled *fixed segments* if the segment represents a recuperation phase (downward slope) or *free segments* if the segment is not representing a recuperation phase. The reason for why the segments are called fixed and free is that when recuperation occurs the algorithm is to recuperate as much energy as possible and the energy flow within the ESS cannot be controlled. If recuperation is not occurring the energy flow within the ESS is free to be controlled by the energy management systems. The dynamic model derived in section 3.1 combined with the conclusions made in subsections 7.1.1 and 7.1.2 are used to predict when the truck will be recuperating energy. The information about where the fix segment starts, the length and the effect on the Soc level is then stored in a matrix,

$$FIX_i = [s_i, \Delta s_i, \Delta SoC_i] \quad (7.4)$$

where  $i$  is the fixed segment number within the present e-Horizon,  $s_i$  is the start of the fixed segment number  $i$ ,  $\Delta s_i$  is the fixed segment length and  $\Delta SoC_i$  is the change in SoC. This is illustrated in Figure 7.4.

Since  $SoC_0$ ,  $s_i$ ,  $\Delta s_i$  and  $\Delta SoC_i$  are known in the *FIX*-matrix the problem is to decide what values  $SoC_i$ ,  $SoC_{i+1}, \dots, SoC_{i+N}$  should have so that the ESS is being used optimally. In other words how can one optimize the trajectory based on the

knowledge of the present position and the information held in the *FIX*-matrix to minimize the fuel consumption. This is done by using *linear programming* which is a fast and powerful algorithm to optimize linear problems. This algorithm will be presented in the next subsection but first some important assumptions are being made about the synthesis of the reference signal [27]:

- Fixed segments are always recuperation intervals where  $\Delta x > 0$ .
- The trajectory always starts in a free segment.
- There can never be two consecutive segments of the same type after each other.

The first assumption says that boosting ( $T_{GB} > \max(T_{ICE})$ ) is not allowed since it is not considered in this text. The second assumption comes from the fact that if the vehicle is in a fixed segment the optimization does not start until the end of this phase according to the definition of fixed and free segments, thus only the free segments are considered as starts for the calculations. The third assumption is how the trajectory is being made [3].

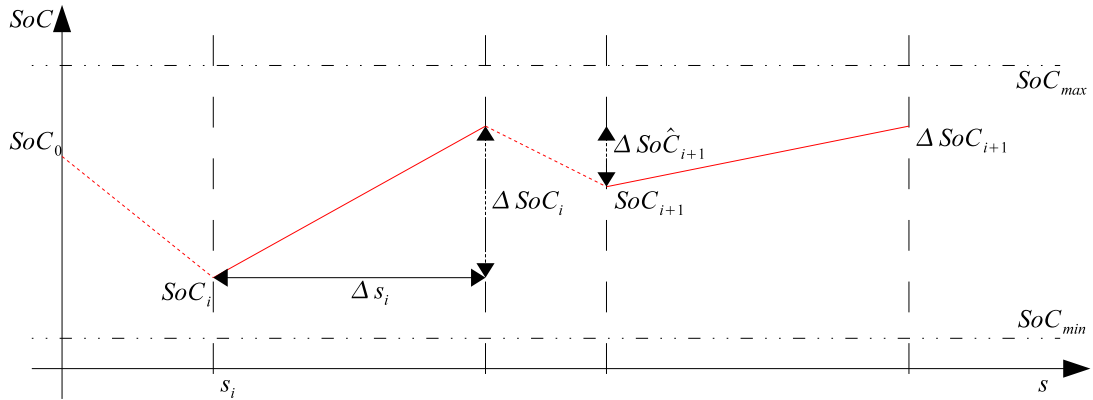


Figure 7.4. Synthesis of the reference signal.  $SoC_0$  is the present  $SoC$  level at present position. From this position an optimization of every free segment is made based on the information of  $\Delta SoC$  in the fixed segments matrix *FIX*. The area between  $SoC_{min}$  and  $SoC_{max}$  is the  $SoC$  window. The unknown variable is  $SoC_i$  which is decided with the estimate  $\Delta \hat{SoC}_i$ .  $\Delta \hat{SoC}_i$  is basically the slope of the free segment trajectory

## Linear Programming

The amount of current drawn from the battery has negative effect on the battery lifetime[3]. Thus an optimization can be constructed based on minimizing the electric current drawn from the battery. Minimizing the current is the same as minimizing the slope of the SoC-trajectory according to

$$\frac{dSoC}{dt} = -\frac{I_{batt}}{Q_0}, \quad (7.5)$$

where  $I_{batt}$  is the current drawn from the battery and  $Q_0$  is the nominal charge of the battery. By using the relation from the equation above a minimizing criteria can be derived for every free segment  $i$ .

$$\begin{aligned} \min_{SoC} \left\{ \sum_{i=1}^N \frac{\Delta \hat{SoC}_i}{\Delta \hat{s}_i} \right\} &= \min_{SoC} \left\{ \sum_{i=1}^N \frac{SoC_i - (SoC_{i-1} + \Delta SoC_{i-1})}{\Delta \hat{s}_i} \right\} = \dots \\ &= \min_{SoC} \left\{ \sum_{i=1}^N \frac{SoC_i - SoC_{i-1}}{\Delta \hat{s}_i} \right\} - \sum_{i=1}^N \frac{\Delta \hat{SoC}_{i-1}}{\Delta \hat{s}_i} \end{aligned} \quad (7.6)$$

where  $SoC$  represent the value which is unknown (refer to figure 7.4),  $\Delta \hat{SoC}_i = SoC_i - (SoC_{i-1} + \Delta SoC_{i-1})$  is the estimate of the SoC change of the free segment and  $\Delta \hat{s}_i = s_i - (s_{i-1} + \Delta s_{i-1})$  is the free segment length<sup>2</sup>.  $\Delta SoC$  is constant so it can be removed from the equation since it does not affect the minimization. Therefore equation (7.7) becomes

$$\min_{SoC} \left\{ \sum_{i=1}^{N-1} \left( \frac{1}{\Delta \hat{s}_i} + \frac{1}{\Delta \hat{s}_{i+1}} \right) SoC_i + \frac{SoC_N}{\Delta \hat{s}_N} \right\} = \min_{SoC} \left\{ \sum_{i=1}^{N-1} c_i SoC_i + c_N SoC_N \right\} \quad (7.7)$$

$$\text{where } c_i = \left( \frac{1}{\Delta \hat{s}_i} + \frac{1}{\Delta \hat{s}_{i+1}} \right) \text{ for } i = 1, 2, \dots, N-1 \text{ and } c_N = \frac{1}{\Delta \hat{s}_N}$$

Since the SoC-window boundary must never be violated, constraints with "slack" variables are introduced

$$\begin{aligned} -SoC_i - \varepsilon_i &\leq -SoC_{min} \\ SoC_i - \varepsilon_i &\leq SoC_{max} - \Delta SoC_i \end{aligned} \quad (7.8)$$

The slack variables exist to make the solution feasible since at some point in time recuperation energy that corresponds to more SoC-change than the window allows can occur. The problem can then be formulated as

<sup>2</sup>In case where there is only a free segment in e-horizon this length will become the e-horizon length.

$$\begin{aligned} & \min_x \sum_i c_i x_i & (7.9) \\ \text{subject to} & \quad A\mathbf{x} \leq \mathbf{b} \end{aligned}$$

$$\text{where } x = (SoC_1 SoC_2 \cdots SoC_N \varepsilon_1 \varepsilon_2 \cdots \varepsilon_N).$$

This problem formulation is in canonical form and can easily be solved with linear programming. When the linear programming algorithm is implemented the problem becomes to implement the pRSG strategy and combine it with the existing ECMS.

### 7.3.2 Implementating the pRSG

The pRSG is implemented in the GSP vehicle model as shown in the figure 7.5 below

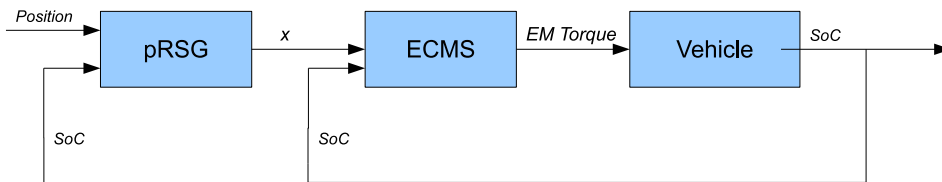


Figure 7.5. Illustration of the implementation of pRSG-ECMS. In this case the P-controller is included inside the ECMS-block. The  $x$ -signal is the SoC-trajectory with which the P-controller calculates an equivalence factor which, together with the present torque demand and the engine speed, will be the input to the ECMS algorithm.

The pRSG block together with the ECMS block builds the *predictive energy management* strategy and is thus called *pRSG-ECMS* in figure 7.5. The reference signal,  $SoC_{ref}$ , is constructed from the e-Horizon data and the *FIX*-matrix together with linear programming, which has been discussed in sub-chapters 7.3.1 and 7.3.1. The implemented pRSG-ECMS is working in two modes:

- when there is no recuperation in sight (mode 1).
- when there is a recuperation phase in sight (mode 2).

When no fixed segments exist within the e-Horizon there will not be any calculations made for the optimal SoC-values since there is no information about the recuperable energy. Instead the reference signal will decay as the EAUX consume power. Mode 1 is illustrated in Figure 7.6, where the reference is kept at a constant slope until recuperation is visible in the e-Horizon.

When there are recuperation phases in the e-Horizon calculations for an optimal trajectory is done by using either linear programming or by just using mode 1. Mode 1 will be used if the optimal value is above the present SoC-value since it is prohibited to steer the reference signal upward which is the same as using the combustion engine as a generator to recharge the ESS. An illustration of this can be seen in Figure 7.7. It is seen that the reference signal drops down to an optimal, or near optimal, value based on the amount of recuperable energy within the e-Horizon.

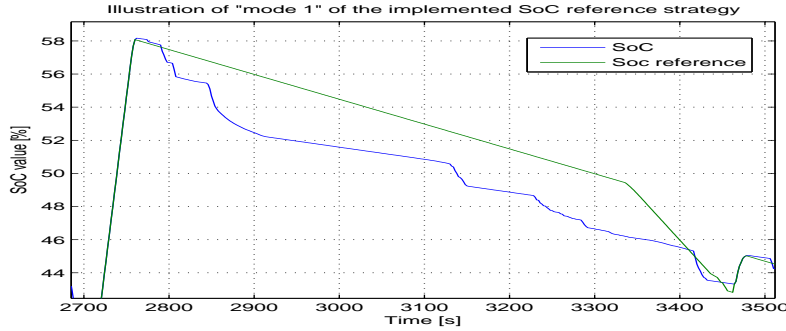


Figure 7.6. This is a figure that illustrates mode 1.

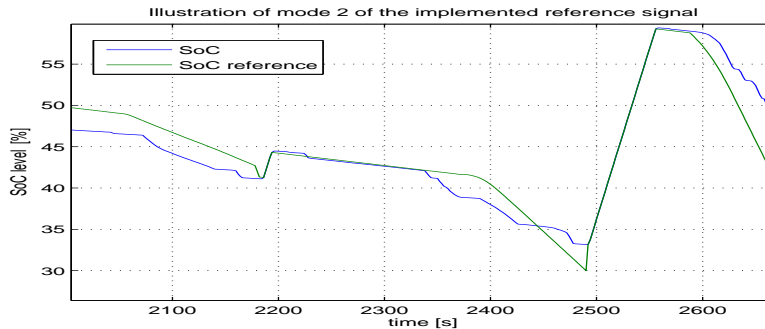


Figure 7.7. This is a figure that illustrates mode 2 (recuperation mode) with constant slope (mode 1). It is seen in figure that when the  $SoC_{ref}$ -value (blue line) is above the  $SoC$ -value the slope is in mode 1 as long as there are no recuperation detected in e-horizon

Mode 1 and mode 2 are based on the information within the e-Horizon and synthesize the SoC-trajectory,  $SoC_{ref}$ , by alternation. The reference signal and the present SoC-value are then used as inputs to the P-controller within the ECMS block where the corresponding equivalence factor (5.11) that was presented in section 5.2 is calculated. This equivalence factor controls the EM in such a way that the right amount of energy is used from the ESS in order to follow the SoC-trajectory.

The P-controller is defined as:

$$s = s_0 + k \cdot \frac{(SoC_{ref}(t) - SoC(t))^{2q-1}}{Q_{nom}V(t)}, \quad (7.10)$$

where  $k$  is a proportional gain,  $s_0$  is the balance factor and  $q$  is a SoC penalty factor that is penalizing large SoC deviations. The balance factor  $s_0$  is used as an equivalence factor when there is no control error, i.e. when the actual SoC-value is the same as the reference signal,  $SoC_{ref}$ .

The parameters in the supervisor have different optimal values depending on the drive-cycle and the hybrid set-up of the truck. The parameters for the P-controller have been tuned for different drive-cycles so that the optimal parameter combination is used for each given cycle. The result from these simulations is presented in Appendix C.

## 7.4 Telemetry Equivalent Consumption Minimization Strategy

One variant of the ECMS-algorithm that evaluates the equivalence factor with respect to past, present and especially *future* driving conditions is the *Telemetry ECMS* (T-ECMS) algorithm [40]. The T-ECMS algorithm calculates the equivalence factor online by using information about the present SoC-value of the ESS, the sum of energies that is needed to drive the vehicle at the set-speeds within the e-Horizon, and the total amount of recuperable energy available within the e-Horizon. With this information a probability-factor,  $p(t)$ , is calculated which weights the equivalence factor between two boundary values,  $S_{dis}$  and  $S_{chg}$ , where  $S_{dis}$  is the upper boundary and  $S_{chg}$  is the lower boundary for the equivalence factor.

The probability factor is formulated as

$$p(t) = \frac{S_{dis}}{S_{dis} + S_{chg}} + \frac{E_e(t) - \Lambda(E_m(t)) \sqrt{S_{dis} + S_{chg}}}{E_m(t) (S_{dis} + S_{chg})}, \quad (7.11)$$

where  $E_e(t)$  is the present amount of available energy within the ESS and  $E_m(t)$  is the total mechanical energy that needs to be delivered to the wheels within the e-Horizon. The parameter  $\Lambda$  is the ratio between the energy that is available for recuperation,  $E_{recup}$  and the mechanical energy that has to be delivered to the wheels,  $E_m(t)$ , within the e-Horizon, i.e.

$$\Lambda = \frac{E_{recup}}{E_m(t)}. \quad (7.12)$$

The equivalence factor is formulated as

$$s(t) = p(t)S_{dis} + (1 - p(t))S_{chg}. \quad (7.13)$$

The energy that is available for recuperation is estimated by using the e-Horizon data presented in section 3.4 and equations provided in section 3.1. Figure 7.8 shows an example of how the equivalence factor is adjusted between two boundary values depending on the distribution of energies and the SoC-level of the ESS.

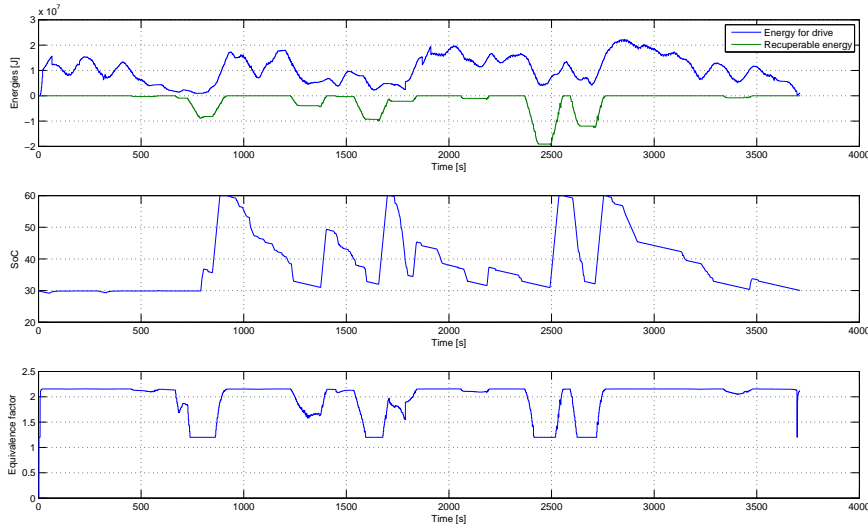


Figure 7.8. Example of how the equivalence factor is adjusted by the T-ECMS strategy. In the top-most graph the blue line represents the energy that is needed to contribute to the wheels ( $E_m(t)$ ) and the green line represents the amount of recuperable energy. The middle graph shows the SoC-curve for the specific drive cycle and the bottom graph shows the resulting equivalence factor. These results are from a simulation on the BLB drive-cycle with a 120 kW EM and 0.6 kWh ESS.

The T-ECMS algorithm offers a simple yet fast algorithm for predictive energy management operations that can compute the equivalence factor (5.11) online and there is no need to store pre-calculated values in look-up tables (except for the ECMS look-up table with the solutions for equation (5.12)).

The disadvantage of this algorithm is that the two boundary parameters  $S_{dis}$  and  $S_{chg}$  have to be tuned in. These tunings are made for a certain vehicle configuration and drive-cycle and such tunings can give robustness problems where  $S_{dis}$  and/or  $S_{chg}$  can change for changed vehicle configurations or road conditions. Robustness problems and results from the tunings will be further discussed in chapter 8. Another disadvantage is that the T-ECMS algorithm is not taking the SoC-window constraints into consideration, which the pRSG-algorithm does. Instead it is assumed that these constraints are indirectly included in the T-ECMS algorithm when the optimal values of  $S_{dis}$  and  $S_{chg}$  are found, since the most fuel-efficient results usually come from parameters that are efficient at avoiding saturations of the battery. This may be seen by the graphs in Figures 7.9 - 7.11. These figures show how the SoC-curve for the BLB drive-cycle differed depending on the choice of  $S_{dis}$  and  $S_{chg}$  parameters.

Figure 7.9 shows the SoC-curve when too low values of the  $S_{dis}$  and  $S_{chg}$  parameters are used. This leads to a low resulting equivalence factor leading to a frequent usage of the EM and the energy within the ESS will be used up quickly. In this case the SoC is often saturated at the lower boundary of the SoC-window and even reaches below the 30%-level which results in that the ICE has to feed the generator (EM) in order to produce enough energy for the EAUX, as explained in section 4.6. Figure 7.10 shows a SoC-curve given by the optimal parameters that were found by tuning. In this graph the SoC saturates at the lower and the upper boundary of the SoC-window at very few instances. Figure 7.11 shows the resulting SoC-curve by using too high values for  $S_{dis}$  and  $S_{chg}$ . In this case the equivalence-factor will in average be relatively high which leads to an underused hybrid system. The energy in the ESS will be used very slowly which leads to many saturations at the upper boundary of the SoC-window.

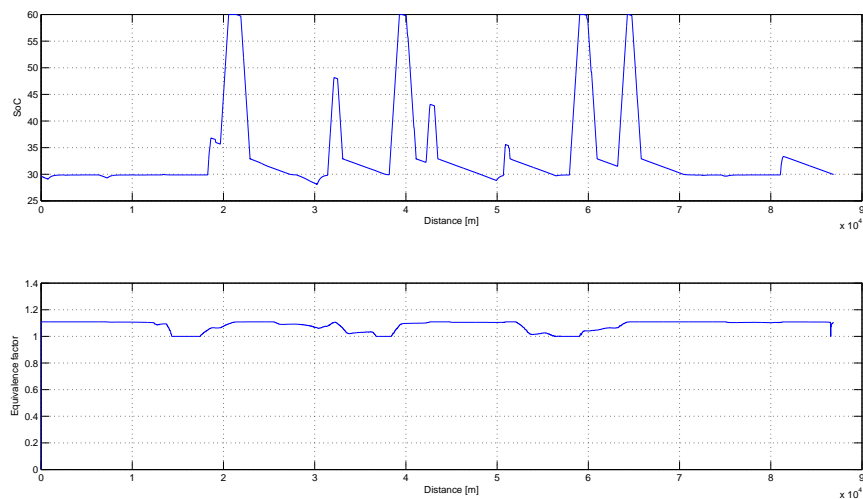


Figure 7.9. Resulting SoC-curve for low values of  $S_{dis}$  and  $S_{chg}$ . The curve reaches the upper boundary of the SoC-window 4 % of the time and the lower boundary 46 % of the time. These results are from a simulation on the BLB drive-cycle with a 120 kW EM and 0.6 kWh ESS.

## 7.5 Constrained T-ECMS

The Constrained T-ECMS (CT-ECMS) algorithm extends the T-ECMS strategy by using the constraints of the ESS that the pRSG strategy delivers. The CT-ECMS algorithm is simply to run both the pRSG- and the T-ECMS strategy and choose the strategy that outputs the lowest equivalence factor at the moment. By doing so, the upper boundary of the SoC-window will not be violated. This may be explained by that if a lower equivalence factor than the pRSG strategy outputs is used more electric energy will be used up from the ESS which takes the actual SoC-value move away from the upper boundary even more, but the lower boundary may still be

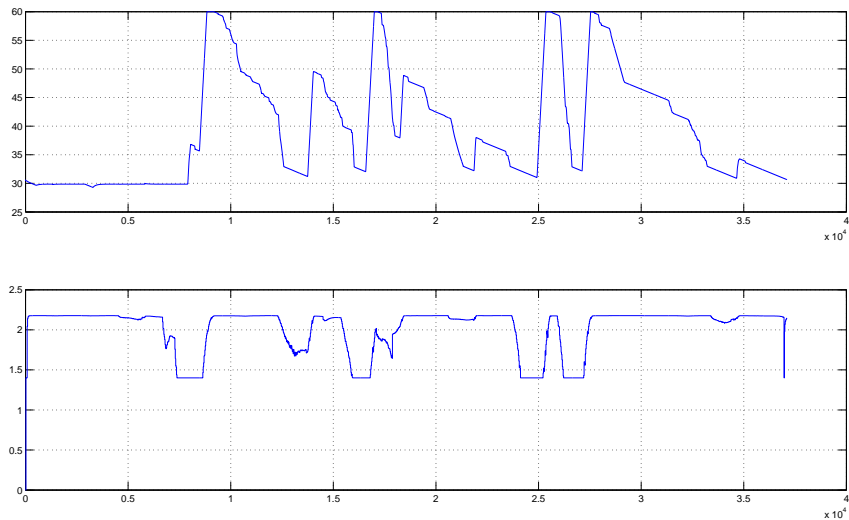


Figure 7.10. Resulting SoC-curve for an optimal choice of the  $S_{dis}$  and  $S_{chg}$  values. The curve reaches the upper boundary of the SoC-window 6 % of the time and the lower boundary 20 % of the time. These results are from a simulation on the BLB drive-cycle with a 120 kW EM and 0.6 kWh ESS.

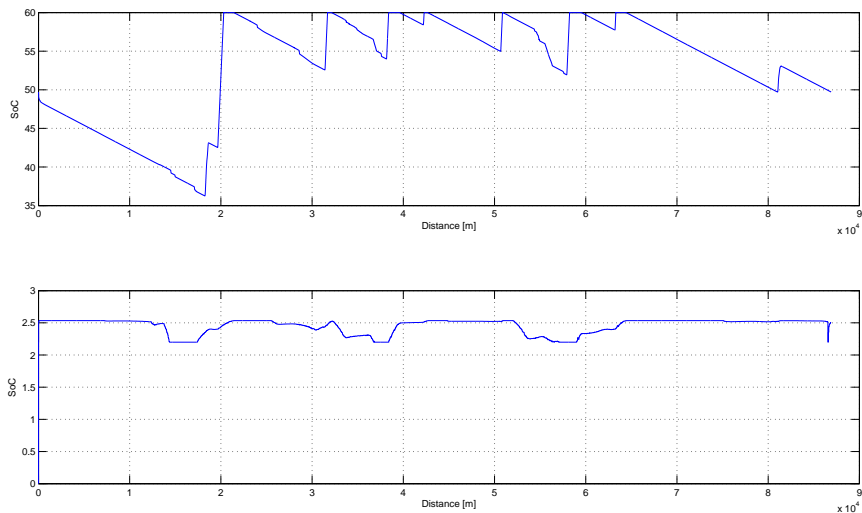


Figure 7.11. Resulting SoC-curve for high values of  $S_{dis}$  and  $S_{chg}$ . The curve reaches the upper boundary of the SoC-window 19.14 % of the time and the lower boundary 0 % of the time. These results are from a simulation on the BLB drive-cycle with a 120 kW EM and 0.6 kWh ESS.

violated (see Figure 7.5). Violations of the lower boundary are not considered as a critical problem, while only violations of the upper boundary lead to losses of recuperable energy, as mentioned in the introduction of this chapter.

Using both the pRSG- and the T-ECMS strategy together would lead to four parameters that have to be tuned in for every drive cycle and hybrid set-up. These are the equivalence boundary values  $S_{dis}$   $S_{chg}$  used within the T-ECMS algorithm and the proportional gain,  $k$ , and the balancing value,  $s_0$ , used for the P-controller within the pRSG algorithm. This leads to an exponential increase in the amount of available combinations between the parameters and the amount of simulations that have to be run, and would therefore not be practically feasible.

To solve this problem the pRSG-block was modified so that instead of having SoC as a function of distance as an output, the output was converted to electric current,  $I$ , as a function of time.  $I$  is the electric current that has to be drained from the EM in order to follow the calculated SoC-trajectory. When the current is known the desired torque output from the EM can easily be calculated by the equality  $T_{EM} = I \cdot U$ , where  $U$  is the ESS voltage and is approximated to be constant. After this modification only the two T-ECMS parameters,  $s_{dis}$  and  $s_{chg}$ , have to be tuned in.

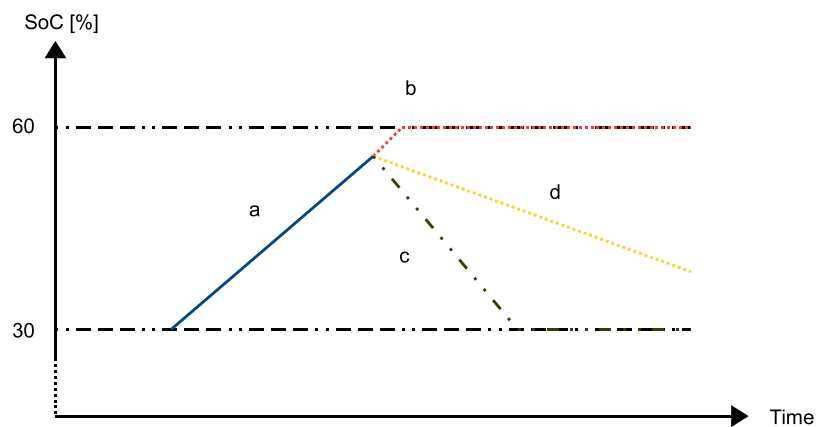


Figure 7.12. The blue line (a) represents the actual SoC-level. The red line (b) represents the resulting SoC-trajectory if an equivalence factor that is higher than the pRSG-strategy outputs is used. The yellow line (d) is the SoC-trajectory achieved by using the equivalence factor from the pRSG strategy. The green line (c) is a resulting SoC-trajectory if a lower equivalence factor than the pRSG outputs is used.

## 8 Results

In this chapter the results for the three different predictive energy management strategies that were developed within this thesis will be presented. Focus will be laid on the hybrid configuration that uses the 120 [kW] electric motor and a battery capacity of 1.35 [kWh], since this configuration has the highest degree of hybridization. If nothing else is mentioned the values from the graphs and tables will be results from this hybrid set-up. For more detailed results, and results from other drive-cycles, see Appendix A. All results are taken from simulations within GSP.

### 8.1 Fuel consumption

Fuel savings of up to 3,98 % can be achieved by the hybrid set-ups used in this work, relative to a conventional truck (Figure 8.1). Figure 8.2 shows the amount of fuel that is saved by using predictive energy management systems compared to the non-predictive energy management system. From these simulation results fuel savings of up to 0.28 % can be achieved by implementing prediction to the control system. An e-Horizon length of 3 kilometers was used for these simulations.

	PL	BLB	SX135
Non-predictive	1,4	3,77	3,81
pRSG	1,55	3,97	3,85
T-ECMS	1,67	3,97	3,98
CT-ECMS	1,37	3,94	3,97

Figure 8.1. Amount of fuel that is saved by using hybrid systems on the different drive-cycles. The rows give the amount of fuel that is saved in percent by using the different energy management systems relative to the conventional truck, where the upper row is the non-predictive energy management strategy already in use by Volvo and the three lower rows are the predictive energy management strategies.

### 8.2 Tunable parameters

In this section the optimal values for the tunable parameters for the T-ECMS strategy and the pRSG strategy will be presented. These parameters are the upper boundary,  $S_{dis}$ , and the lower boundary,  $S_{chg}$ , for the equivalence factor within the T-ECMS strategy, and the balance factor,  $s_0$ , and the proportional gain factor,  $k$ , for the P-regulator within the pRSG strategy. The optimal values are given in table 8.2. How these values were found is explained in Appendix C.

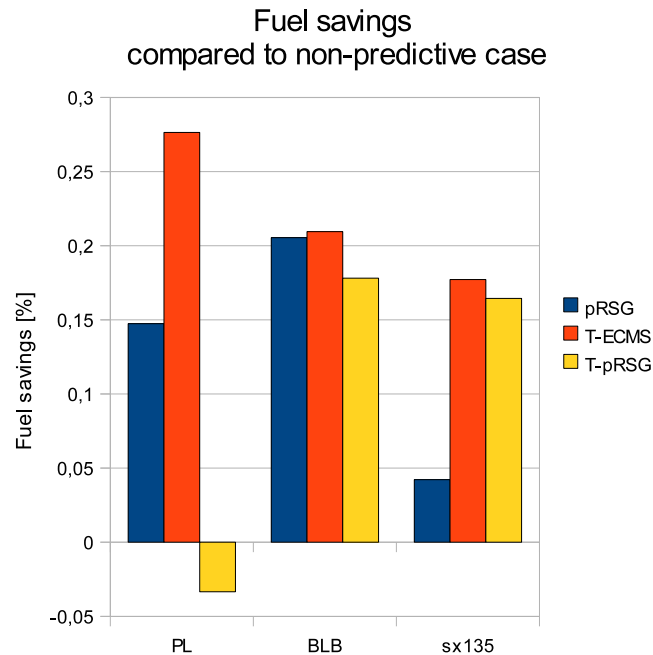


Figure 8.2. The bars indicate the amount of fuel that can be saved by using predictive energy management strategies, compared to the non-predictive strategy. All values yield for the hybrid configuration with a 120 kW motor and a 1.35 kWh battery capacity.

Strategy	Drive cycle	k	$s_0$
pRSG	BLB	2,1	0,2
	PL	1,4	0,2
	sx135	1,7	0,1
T-ECMS		<b>Sdis</b>	<b>Schg</b>
	BLB	1,8	2,4
	PL	1,8	2,2
	sx135	2,2	1,6

Figure 8.3. Optimal tunable parameters for the hybrid set-up with a 120 kW and 1.35 kWh battery capacity.

## 8.3 Drivability

Drivability defines the empirical experience of how an actual real-life vehicle feels like to drive, for example concerning the smoothness of the drive and pedal response. Estimating drivability factors from software simulations can be accomplished in many different ways, but none of them is comprehensive [18]. In this section an attempt will be made in trying to answer how the predictive torque-split control affects the drivability.

Different parameters related to drivability, may be estimated depending on the required accuracy of the drivability estimation. A criterion for these parameters is that they can be calculated from the GSP simulation results. All values will be compared to both the non-predictive energy management strategy and the conventional truck. Three such parameters were selected and used for the vehicle drivability approximation; speed difference from the set-speed, average vehicle speed and the number of gearshifts during a drive-cycle.

First, a calculation for the percentage of which the actual speed differed from the set-speed was made. A tolerance value was used for how much speed difference that was acceptable. The tolerance value was set to be the same as in [18], which is 3 [km/h]. Only speeds differences than were lower than the set-speed were considered. The calculations would thus show how often the actual speed of the vehicle was below the set-speed by at least 3 [km/h]. This difference mainly arises as the vehicle accelerates, which is why this parameter also can be used to describe the acceleration performance of the truck. The difference in vehicle speed,  $v_{diff}$ , was calculated as

$$v_{diff} = v_{set} - v_{act} \quad (8.1)$$

were  $v_{set}$  is the set speed of the road and  $v_{act}$  is the actual speed of the vehicle. The acceleration in the beginning of the drive-cycle was not included in these calculations. That kind of accelerations are usually given in the vehicle data sheets as the time it takes for the vehicle to accelerate from 0 [km/h] up to 100 [km/h]. These calculations will instead show the overall acceleration performance while the vehicle is utilized. The percentage of which the speed differed at least 3 [km/h] from the set-speed was then calculated in Matlab. Figure 8.4 lists the results from these calculations for the different road cycles. There will not be any significant deviations from the set-speed since the EECU always tries to fulfill the constraint (4.3). However there may be instances when the constraint cannot be fulfilled. This speed-loss can result from two factors: as a transient from the driver which is modeled as a PI-regulator and/or when the torque demand on the wheels exceeds the maximum torque-output available from the vehicle (see Figure 8.6). In case of the transient the set-speed will be achieved after the settling time but in case when the maximal torque-output from the vehicle is not enough the speed-difference will remain as long as the torque demand cannot be met. The correlation between uphill and speed-loss becomes especially clear in figure 8.5 where a comparison is made between the  $v_{diff}$  and the average road gradient.

The second drivability investigation concerns the average speed, which is defined as

$$v_{avg} = \frac{Distance_{cycle}}{Time_{cycle}} \quad (8.2)$$

This parameter shows if the predictive energy management strategies have some influence on the time it takes to drive through the given drive-cycle. One way to

Drive-cycle	PL	BLB	sx135
Time below set-speed [%]	0,3	6,86	22,07

Figure 8.4. Amount of time the actual speed is at least 3 [km/h] below the set-speed.

decrease the fuel consumption would be to decrease the speed of the vehicle which in equation (3.2) would lead to less air resistance force acting on the chassis of the truck and therefore also less fuel consumption. This is however unwanted since it leads to longer traveling times, therefore the average speed has to be held as close as possible to the set-speed. Figure 8.7 lists the results from the average speed for different hybrid set-ups and road cycles. What is interesting is that the average speed of the hybrid truck is higher than the conventional truck, regardless of which energy management strategy is used. This may be explained by the extra power-output delivered to the powertrain from the EM which gives a higher combined torque-output in phases that require more torque than the ICE can deliver. It is obvious that the average speed of a whole drive-cycle depends very much on the ability of the vehicle to hold the set-speed, that is, to have a minimum of  $v_{diff}$ .

The predictive energy management strategies did not affect the amount of gearshifts at all.

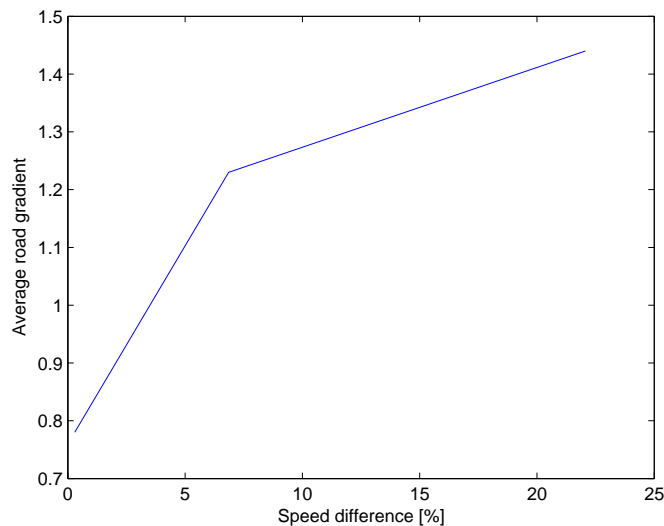


Figure 8.5. Percentual difference with at least 3 [km/h] beneath the set-speed and average road gradient. It can be seen that the average road gradient has a big influence on the amount of time that the vehicle spends at lower speeds than the set-speed.

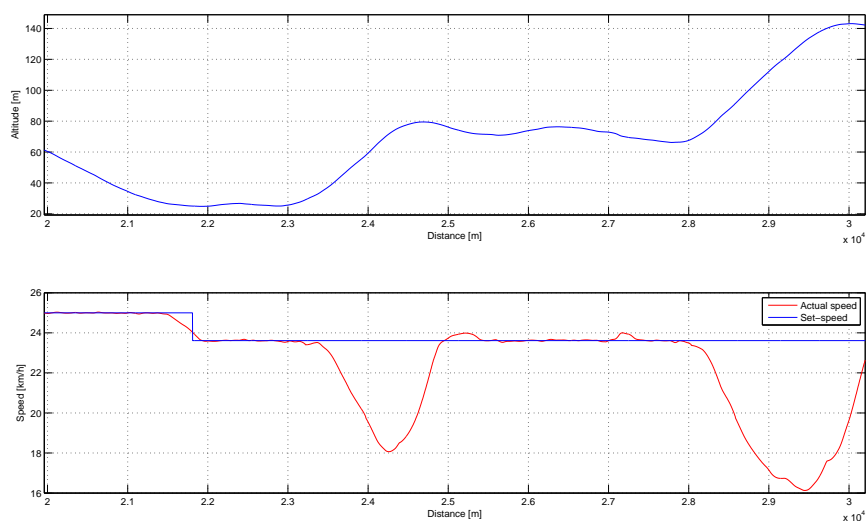


Figure 8.6. Example of speed-loss at uphill. When the truck starts driving at steep uphill it is affected by a speed-loss.

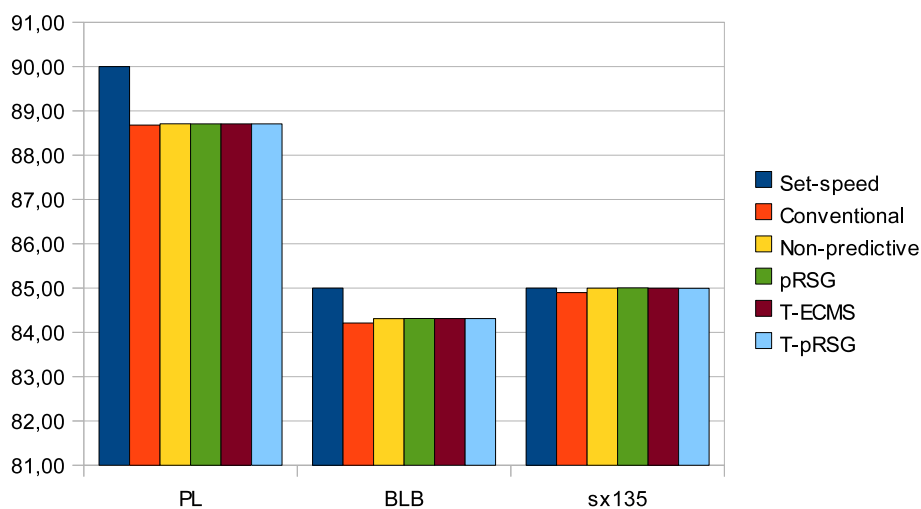


Figure 8.7. The set-speed and the average speeds achieved by the trucks for the different drive-cycles. The hybrid trucks have a hybrid set-up with a 1.35 [kW] battery and a 120 [kW] EM.

## 8.4 Effects from changes in the e-Horizon length

This section aims at giving the reader an overview of the possible benefits of extending the preview horizon. Simulations were done where the preview horizon was extended from 3 kilometers to 6 kilometers. In case of the T-ECMS strategy the improvement differences on the fuel consumption were small enough to be neglected since they could be results from errors in the parameter tuning. It was however

noticed that the optimal values of the  $S_{dis}$  and  $S_{chg}$  parameters changed. In case of the pRSG strategy there were improvements when the preview horizon was extended. The optimal values of the gain- and balancing factor changed and had to be re-tuned. Figure 8.8 shows the improvement in fuel economy in percent for the pRSG strategy.

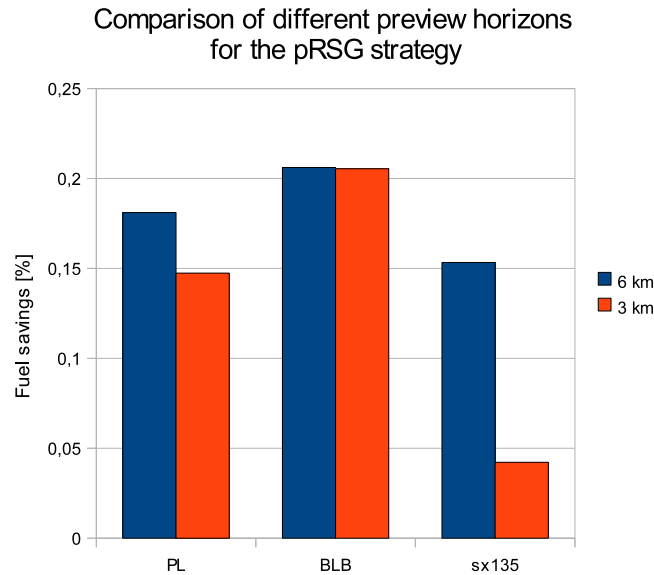


Figure 8.8. Fuel savings using the pRSG strategy with two different preview lengths. Comparisons are relative to the non-predictive algorithm.

## 9 Discussion

In this chapter the results from the previous chapter will be discussed and analyzed.

### 9.1 Fuel consumption

	PL	BLB	sx135
Fuel saving [%]	1,55	3,97	3,85
Average road gradient [%]	0,78	1,23	1,44

Figure 9.1. Average road gradients and achieved fuel savings on different drive-cycles. Comparisons are made on the conventional truck.

Simulations indicate that it is possible to improve the fuel economy for a mild hybrid long haul truck with the predictive control algorithms developed within this thesis work. The amount of fuel that can be saved depends on different factors, such as maximum output power from the electric motor, battery capacity, e-Horizon scope, and the average road gradient. The average road gradient has most influence on the fuel economy, where a high road gradient leads to more recuperation and thus more fuel savings. The average road gradients for the three drive-cycles and the amount of fuel that was saved on each drive-cycle are given in Figure 9.1. Drive cycle sx135 had the highest average road gradient but surprisingly the amount of fuel that is saved is not as high as for the BLB drive-cycle which has a lower average road gradient. Of the configurable factors that can be influenced on the power-output from the electric motor has slightly more impact on the fuel economy than the battery capacity has, as can be seen in Figure 9.2. An electric motor with higher power-output will give more recuperation <sup>1</sup>.

In the simulations carried out the less advanced T-ECMS strategy behaved better than the more advanced pRSG strategy, from a fuel-consumption point of view.

### 9.2 Parameters

Both the T-ECMS strategy and the pRSG strategy are using parameters that have to be tuned for all the different hybrid set-ups and also for the different drive-cycles, respectively. For more information about how the tuning was carried out and the results for the optimal parameters, see Appendix C. The sensitiveness to

---

<sup>1</sup>This statement is based on the battery capacities and the electric motor sizes that has been defined for this thesis work.

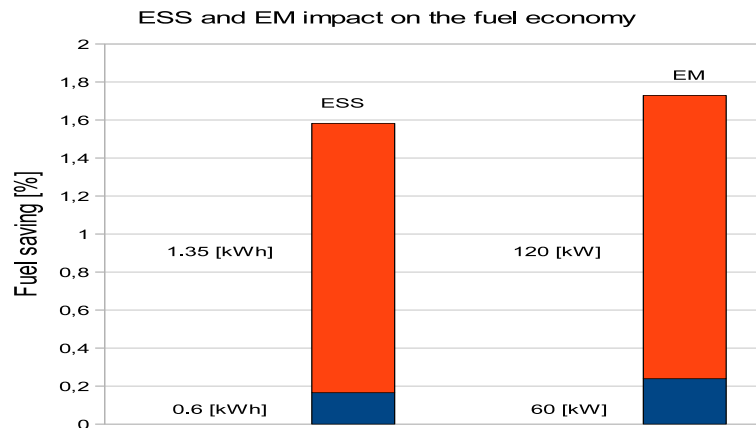


Figure 9.2. The left-most bar indicate the amount of fuel that is saved when the electric motor is held constant and the ESS capacity is changed. The right-most bar indicate how the fuel economy is affected by changing the maximum input and output power from the EM. All values are taken for the BLB drive-cycle and the comparisons are made with a conventional truck.

changes in drive-cycles is seen as more important than the sensitiveness to changes in hybrid set-ups within the truck. This is because the hybrid set-up will be held constant for a given truck while the driving environment will be changing<sup>2</sup>. A robustness analysis was done by taking the combination of parameters that gave the lowest *total* fuel consumption for the three drive-cycles for a certain hybrid set-up. This combination of parameters can be seen as the best average parameters for drive-cycles with different average road gradients. Figure 9.3 show the amount of fuel that is saved using the optimal parameters for the drive-cycles and using the average parameters, respectively. Also with these average parameters there was an improvement compared to the non-predictive case.

## 9.3 Horizon change

When the horizon length was extended to 6 kilometers there were no improvements in the fuel economy for the T-ECMS strategy. The upper boundary,  $S_{dis}$ , and lower boundary,  $S_{chg}$ , for the equivalence factor where however changed with the preview horizon length. In case of the pRSG strategy there were minor improvements in the fuel economy when the preview horizon was extended from 3 kilometers to 6 kilometers. These improvements are due to the fact that there will be more information about the future road topography with an extended horizon and the pRSG strategy can compute a better SoC-reference curve using this information. When the horizon length was changed there was a minor change to the optimal gain parameter,  $k$ , and the balancing factor,  $s_0$ . Figure 9.4 shows a comparison on

<sup>2</sup>If a truck is driving a certain route frequently the tunable parameters may be optimized for that given route.

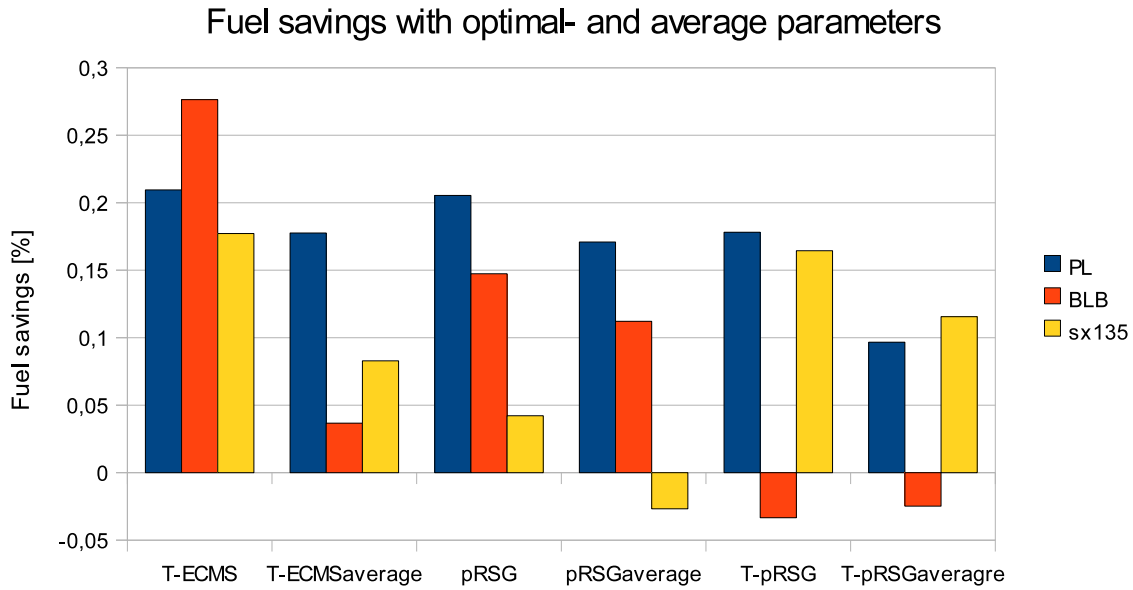


Figure 9.3. Fuel savings when using optimal and average tunable parameters. All values are taken from a hybrid set-up with a 120 kW motor and a 1.35 kWh battery capacity. Comparisons are made on the non-predictive energy management strategy.

how much fuel that is saved with the different preview horizons, compared to the non-predictive strategy.

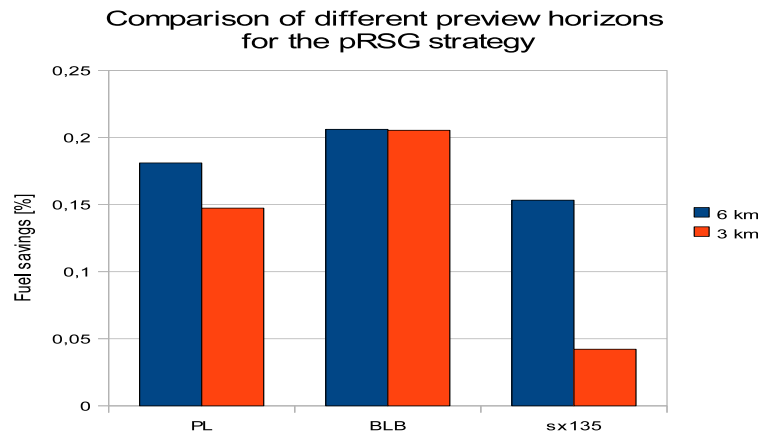


Figure 9.4. The bars indicate the amount of fuel that is saved compared to the non-predictive strategy by using the pRSG strategy with preview horizons of 3 kilometers and 6 kilometers. A preview horizon of 6 kilometers give better results on all three drive-cycles.

## 10 Future work

The time constraints of this thesis project naturally limits the number of investigations that can be done on how to improve the fuel efficiency of the long haul truck. A few methods will be described below that could possibly improve the fuel efficiency even more. Also a short analysis of why these methods are believed to improve the fuel efficiency will be given.

First of all it may be wise to test the efficiency of the predictive EMS in reducing fuel consumption against the most fuel efficient predictive strategy that is possible to get, one that gives a global minimum in fuel consumption. Such an optimal strategy can be obtained by dynamical programming. That kind of test would show how well the energy management strategies really perform and how much the torque-split can be further enhanced.

The prediction based strategies could also be further enhanced by implementing algorithms that include various vehicle stops and speed-decreases in the optimization process. The strategies presented in this paper cannot handle this in an optimal manner. If these strategies are to be implemented in a real vehicle it may also be wise to implement algorithms that can handle speed-decreases due to for example hard turns in the road. The drive cycles within GSP do not include turns and the routes are therefore approximated as straight roads. Including vehicle stops and speed-decreases would give a more fair value of the recuperable energy within the e-Horizon which would lead to a better optimization process.

A strategy which could further improve the fuel efficiency of the truck is to combine *ZeroPedal* with the predictive EMS. *ZeroPedal* is a strategy already in use by many Volvo trucks where the fuel injection to the engine is stopped in downhill slopes. Since the gravity pulls the truck down the slope the engine is cranked by the momentum of the vehicle. The benefit of using *ZeroPedal* is that no fuel is consumed. The disadvantage is that the inner engine friction causes a small retarding force leading to a waste of energy. When used with predictive EMS, *ZeroPedal* could be deployed when the battery or the EM is saturated, i.e. when the vehicle is in a very long or very steep downhill.

Another possible strategy is to combine the predictive EMS with *EcoRoll*. *EcoRoll* is a function developed by Volvo which reminds of *ZeroPedal* but in which the gear is shifted to neutral. Shifting the gear to neutral decouples the engine from the powertrain which reduces the retarding force considerably. The lower retarding force allows the vehicle to better convert the potential energy into kinetic energy making the vehicle roll further after the downhill. The disadvantage of this function is that since the engine is decoupled from the powertrain it has to be maintained at idle speed which consumes a small amount of fuel. This function may be implemented together with the predictive EMS for the same reasons as for the *ZeroPedal* function described above.



# Bibliography

- [1] NRC (2008). Understanding and responding to climate change. Technical report, Board on Atmospheric Sciences and Climate, US National Academy of Sciences, 2008.
- [2] M. Back A. Sciartta and L. Guzzella. Optimal control of parallel hybrid electric vehicles. *IEEE Transactions on Control Systems Technology*, 12(3):352–363, 2004.
- [3] D. Ambühl and L. Guzzella. Predictive reference signal generator for hybrid vehicles. *IEEE Transactions on Vehicular Technology*, 2009.
- [4] B. Staccia C. Musardo, G. Rizzoni. A-ecms: an adaptive algorithm for hybrid electric vehicle energy management. In *A-ECMS: an adaptive algorithm for hybrid electric vehicle energy management*, volume 44. Proc. of the 44th IEEE Conf. on Decision and Control, and the 2005 European Control Conference, 2005.
- [5] Confidential. Simulations for p3611 mild hybrid for demanding long haul. Volvo Engineering Report, 2009.
- [6] I. Romieu et al. Air pollution, oxidative stress and dietary supplementation: A review. *European Respiratory Journal*, 31(179), 2008.
- [7] M. Geiser et al. Ultrafine particles cross cellular membranes by nonphagocytic mechanisms in lungs and in cultured cells. *Environmental Health Perspectives*, 113(11):1555-1560, 2005.
- [8] O. Günter et al. Nanotoxicology: An emerging discipline evolving from studies of ultrafine particles. *Environmental Health Perspectives*, 113:823-839, 2005.
- [9] S. Radoslav et al. Micellar nanocontainers distribute to defined cytoplasmic organelles. *Science*, 300(5619):615-618, 2003.
- [10] T. Osunsanya et al. Acute respiratory effects of particles: mass or number? *Occupational Environmental Medicine*, 58(154), 2001.
- [11] B. Daran CC. Lin-U. Yildir B. Wu M. Kokkolaras D. Assanis H. Peng P. Papalambros J. Stein D. Szkubiel R. Chapp F. Filipi, L. Louca. Combined optimisation of design and power management of the hydraulic hybrid propulsion-system for the 6 times 6 medium truck. *International Journal of Heavy Vehicle Systems*, 11(3):371–401, 2004.
- [12] World Wide Fund for nature (WWF). Klimatfrågan lösningar, 2005.
- [13] A. Brahma Y. Guezennec G. Paganelli, G. Ercole and G. Rizzoni. General supervisory control policy for the energy optimization of charge-sustaining hybrid electric vehicles. *Special Issue of JSAE Review*, 22(4):511–518, 2001.

- [14] S. Delprat J.-J. Santin M. Delhom G. Paganelli, T.-M. Guerra and E. Combes. Simulation and assessment of power control strategies for a parallel hybrid car. *Proc. IMechE, Part D: J. Auto. Eng.*, 214(7):705–717, 2000.
- [15] T. Glad and L. Ljung, editors. *Control Theory, Multivariable and Nonlinear Methods*. Taylor & Francis Group, 2000 N.W. Corporate Blvd, Boca Raton, Florida 33431, 1st edition, 2000.
- [16] G.Rizzoni G.Paganelli, A.Brahma and Y.Guezennec. Control development for a hybrid-electric sport-utility vehicle: strategy, implementation and field test results. American Control Conference, 2001.
- [17] R. Grahn and P.Å. Jansson, editors. *Mekanik, Statik och Dynamik*. Studentlitteratur, Sweden, 2nd edition, 1997.
- [18] J. Gustafsson. Analysis and simulation of fuel consumption and energy throughput on a parallel diesel-electric hybrid powertrain. Master’s thesis, Division of Electric Power Engineering, Chalmers University of Technology, 2009.
- [19] L. Guzzella and A. Sciarretta, editors. *Vehicle Propulsion Systems, Introduction to Modeling and Optimization*. Springer-Verlag, Germany, 1st edition, 2005.
- [20] Energitillfrseln internationellt. Ekonomifakta, 2010-06-16.
- [21] J. Wettestad J.B. Skjaereth. Is eu enlargement bad for environmental policy? confronting gloomy expectations with evidence. *International Environmental Agreements, Fridtjof Nansen Institute*, 2007.
- [22] James C. Bonner Jeffrey W. Card, Darryl C. Zeldin and Earle R. Nestmann. Pulmonary applications and toxicity of engineered nanoparticles. *American Journal of Physiology and Lung Cell Molecular Physiology*, 295, 2008.
- [23] L. Johannesson. *Predictive control of hybrid electric vehicles on prescribed routes*. PhD thesis, Chalmers University of Technology, SE-412 96 Göteborg, Sweden, 2009. ISBN 9789173852630.
- [24] N. Johansson and O. Klintenberg. Preview-information-based transmission functions for improved fuel economy in heavy trucks. Master’s thesis, department of signals and systems, Chalmers University of Technology, 2008.
- [25] G. Tyler Miller Jr., editor. *Living in the environment*. Thomson Brooks/Cole, USA, 5th edition, 2007.
- [26] DW. Hornung K. Steenland, DT. Silverman. Case control study of lung cancer and truck driving in the teamsters union. *American Journal of Public Health*, 80:670–674, 1990.
- [27] H. Karloff, editor. *Linear Programming*. Birkhäuser Boston, US, 1st edition, 1991.

- [28] E. Karlsson and M. Wilner. Analysis of hybrid management strategies. Master's thesis, Department of signals and systems Division of Automatic Control, Automation and Mechatronics, Chalmers University of Technology, 2008.
- [29] A. Kleimaier and D. Schrder. An approach for the online optimized control of a hybrid powertrain. In *An approach for the online optimized control of a hybrid powertrain*, pages 215–220. 7th Int. Workshop Advanced Motion Control, 2002.
- [30] et.al Lilian Calderon-Garciduenas. Long-term air pollution exposure is associated with neuroinflammation, an altered innate immune response, disruption of the blood-brain barrier, ultrafine particulate deposition, and accumulation of amyloid b-42 and a-synuclein in children and young adults. *Toxicologic Pathology*, 36(298), 2008.
- [31] C. Monforton. Weight of the evidence or wait for the evidence? protecting underground miners from diesel particulate matter. *American Journal of Public Health*, 96:271–276, 2006.
- [32] D. Naidu, editor. *Optimal Control Systems*. CRC PRESS, 29 West 35th Street, New York, NY 10001, 1st edition, 2002.
- [33] National Energy Information Center (NEIC). Greenhouse gases, climate change, and energy.
- [34] N. Oreskes. Beyond the ivory tower: The scientific consensus on climate change. *Science*, 306(5702), 2004.
- [35] R.K. Pachauri and A. Reisinger. Summary for policymakers:observed changes in climate and their effects. In *Climate Change 2007: Synthesis Report. Contribution of Working Groups I, II and III to the Fourth Assessment Report of the Intergovernmental Panel on Climate Change*. IPCC, Geneva, Switzerland, 2007.
- [36] Lisa Gahagan Paul Mann and Mark B. Gordon. Tectonic setting of the worlds giant oil and gas fields. In Michel T. Halbouty, editor, *Giant Oil and Gas Fields of the Decade - 1990-99, Volume 78*. American Association Of Petroleum Geologists, Tulsa, Okla., 1st edition, 2004.
- [37] Proc. of the IFAC Symposium on Advances in Automotive Control. *Real-time optimal control strategy for parallel hybrid vehicles with on-board estimation of the control parameters*, 2004.
- [38] T.M. Guerra S. Delprat, J. Lauber and J. Rimaux. Control of a parallel hybrid powertrain: optimal control. *IEEE Trans. Veh. Technol.*, 53(3):872–881, 2004.
- [39] et.al S. Solomon, D. Qin. Summary for policymakers. in: Climate change 2007: The physical science basis. contribution of working group i to the fourth assessment report of the intergovernmental panel on climate change. Technical report, IPCC, Cambridge University Press, Cambridge, United Kingdom and New York, NY, USA, 2007.

- 
- [40] A. Sciartta and L. Guzzella. Control of hybrid electric vehicles. *IEEE Control Systems Magazine*, April 2007:60–70, 2007.
- [41] J. Slingo. Explaining the evidence of climate change.
- [42] U.S. EIA International Energy Statistics. International energy statistics.
- [43] G. Steinmauer and L. del Re. Optimal control of dual power sources. In *Optimal control of dual power sources*, pages 422–442. IEEE Int. Conf. Control Applications, 2001.
- [44] K. Teichman. Notice of availability of the nanomaterial research strategy external review draft and expert peer review meeting. *Federal Register*, 73(30), 2008.
- [45] W. Müller W.G. Kreyling, M. Semmler-Behnke. Ultrafine particle-lung interactions: does size matter? *Journal of Aerosol Medicine*, 19(1), 2006.
- [46] H.-E. Wichmann. Abschätzung positiver gesundheitlicher Auswirkungen durch den Einsatz von Partikelfiltern bei Dieselfahrzeugen in Deutschland. *Umweltbundesamt Berlin*, 2352:32, 2003.
- [47] H.-E. Wichmann. Future diesel. Abgasgesetzgebung PKW, leichte NFZ und LKW Fortschreibung der Grenzwerte bei Dieselfahrzeugen. *Umweltbundesamt Berlin*, 2353:25, 2003.
- [48] the free encyclopedia Wikipedia. Optimal control.

# Appendix A

## Fuel consumption Results

app:appfuel

In this chapter detailed results of the fuel consumptions from all the drive-cycles and the different hybrid set-ups will be presented. Many of the simulation-values are confidential within the Volvo Group and the results will therefore be given as change in percent with respect to either a conventional truck or the non-predictive hybrid truck. The performance of a conventional truck has the same advantage for all of the drive-cycles and therefore gives a good benchmark of how well the predictive energy management strategies behave, from a fuel consumption point of view. The gain-and balance factor of the non-predictive algorithm presented in chapter 6 has been tuned in such a way that they behave better on some of the drive-cycles. Therefore the comparison between the non-predictive and the predictive energy management strategies only gives information of how much fuel that can further be saved by using prediction.

EM	Drive cycle	Conventional Truck	Non-predictive strategy
120 kW	PL	1,55	0,15
	BLB	3,97	0,21
	sx135	3,85	0,04
60 kW	PL	1,05	0,22
	BLB	2,48	0,15
	sx135	2,59	0,1
120 kW	PL	1,09	0,08
	BLB	2,55	0,15
	sx135	2,42	0,11
60 kW	PL	0,84	0,1
	BLB	2,31	0,16
	sx135	2,15	0,1

Figure A.1. Fuel savings achieved by using the pRSG strategy compared to a conventional truck and a hybrid truck using the present non-predictive energy management strategy.

EM	Drive cycle	Conventional truck	Non-predictive strategy
120 kW	PL	1,67	0,28
	BLB	3,99	0,23
	sx135	3,98	0,18
60 kW	PL	1,06	0,22
	BLB	2,54	0,21
	sx135	2,72	0,14
120 kW	PL	1,27	0,27
	BLB	2,6	0,2
	sx135	2,49	0,18
60 kW	PL	0,98	0,24
	BLB	2,32	0,17
	sx135	2,15	0,1

Figure A.2. Fuel savings achieved by using the T-ECMS strategy compared to a conventional truck and a hybrid truck using the present non-predictive energy management strategy.

EM	Drive cycle	Conventional Truck	Non-predictive strategy
120 kW	PL	1,4	0
	BLB	3,91	0,14
	sx135	3,96	0,16
60 kW	PL	0,83	0
	BLB	2,42	0,1
	sx135	2,73	0,14
120 kW	PL	-1,3	-2,32
	BLB	2,58	0,18
	sx135	2,43	0,13
60 kW	PL	0,68	-0,06
	BLB	2,28	0,13
	sx135	2,17	0,12

Figure A.3. Fuel savings achieved by using the CT-ECMS strategy compared to a conventional truck and a hybrid truck using the present non-predictive energy management strategy.

## Appendix B

### Change in the average vehicle speed

app:appavgspeed

Figure B.1 shows the set-speed and the average speed obtained by the different truck for different drive-cycles. For the PL and BLB drive-cycles the obtained average speed is lower than the set-speed for all the trucks, but the performance is improved when using hybrid systems. It does not seem like predictive energy management strategies has a benefit over non-predictive strategies in this case.

Drive cycle	Conventional truck	Non-predictive strategy	pRSG	Tecms	T-pRSG	Set-speed
PL	88,68	88,71	88,71	88,71	88,71	90
BLB	84,21	84,31	84,31	84,31	84,31	85
sx135	84,90	85,00	85,00	85,00	84,99	85
PL	88,68	88,71	88,71	88,71	88,71	90
BLB	84,21	84,31	84,31	84,31	84,32	85
sx135	84,90	85,00	85,00	85,00	85,01	85
PL	88,68	88,71	88,71	88,71	84,31	90
BLB	84,21	84,31	84,31	84,31	84,31	85
sx135	84,90	85,00	85,00	85,01	85,00	85
PL	88,68	88,72	88,71	88,71	88,71	90
BLB	84,21	84,31	84,32	84,31	84,31	85
sx135	84,90	85,00	85,00	85,01	85,01	85

Figure B.1. Average speeds for a conventional truck and trucks using the different energy management strategies. The four different row-sections define the degree of hybridization where the row-section from top to bottom represents the following; 60 kW EM and 0.6 kWh ESS, 120 kW EM and 0.6 kWh ESS, 60 kW EM and 1.35 kWh ESS, 120 kW EM and 1.35 kWh ESS.



## Appendix C

# Tuning of the T-ECMS and pRSG parameters

app:tuning

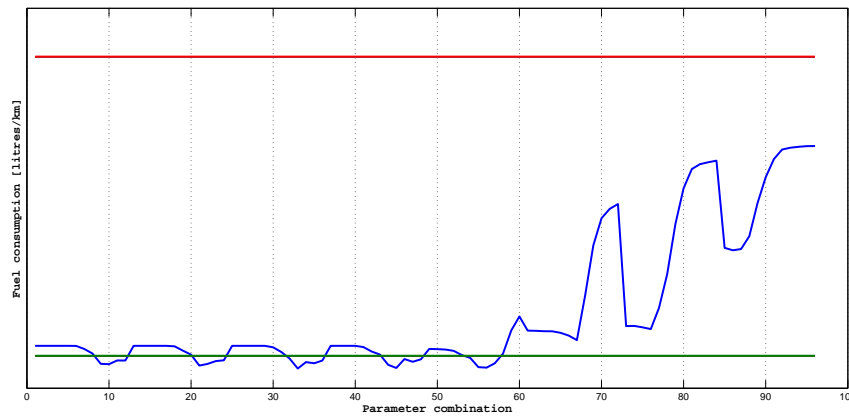


Figure C.1. A tuning example. The blue line is the total fuel consumption for the BLB drive cycle using a 1.35 kWh battery and 120 kW EM. The line was built up by 96 different parameter combinations between  $S_{dis}$  and  $S_{chg}$ . The red ellipse represents a local minimum around which further and more narrow tunings were made with a smaller step-size,  $\Delta$ . The red line represents the fuel consumption for the conventional vehicle and the green line represents the fuel consumption resulted from the non-predictive hybrid truck.

The T-ECMS strategy and the pRSG strategy use parameters that have to be tuned in to some optimal value for a given hybrid set-up and drive-cycle. These parameters are the two boundary parameters,  $S_{dis}$  and  $S_{chg}$ , for the T-ECMS strategy and the balancing factor and gain,  $b$  and  $k$ , for the P-regulator within the pRSG strategy.

The tuning process is quite simple. First a range of increasing values is chosen for the parameters, ( $S_{dis} = [sd_0, sd_f]$ ,  $S_{chg} = [sc_0, sc_f]$  and  $b = [b_0, b_f]$ ,  $k = [k_0, k_f]$ ), where the increment in each set depends on a predefined step-size ( $\Delta S_{dis}$ ,  $\Delta S_{chg}$  etcetera). Then simulations are run for every combination of  $S_{dis}$  and  $S_{chg}$  for

the T-ECMS algorithm and  $k$  and  $b$  for the pRSG algorithm. By comparing the simulation results for all the combinations the combination that gave the best results for a certain data can be chosen. Due to the objective of this thesis, to investigate if better fuel economy can be achieved by using predictive energy management, the combination that gave the lowest fuel consumption where chosen. Figure C.1 shows a tuning example from the BLB drive cycle. The blue line represents the total fuel consumption as a function of the parameter combinations. In this case a total of 96 combinations between  $S_{dis}$  and  $S_{chg}$  were used and therefore the same amount of simulations had to be run. The red ellipse represents a local minimum in fuel consumption. Around all these local minima further tunings were done with a smaller step-size,  $\Delta$ . The smaller step-size was only used on the  $S_{dis}$  parameter while narrower tunings of  $S_{chg}$  were not made.

Both the T-ECMS strategy and the pRSG strategy have two parameters each that have to be tuned. If the amount of values within the range of these two parameters are the same, that is if  $size([sd_0, sd_f]) = size([sc_0, sc_f])$  and  $size([b_0, b_f]) = size([k_0, k_f])$ , the amount of combinations will be square the amount of values within the range. The optimal parameter values can be found in figure C.2 and C.3.

Battery capacity	MDS	Drive cycle	Sdis	Schg
1350 Wh	120 kW	BLB	2,6	1,4
		PL	1,8	2,2
		sx135	2,2	1,6
	60 kW	BLB	1,8	2,4
		PL	1,8	2,2
		sx135	2,2	1,6
600 Wh	120 kW	BLB	2,6	1,4
		PL	1,6	2,4
		sx135	2,2	1,8
	60 kW	BLB	2,6	1,4
		PL	2,4	2,4
		sx135	2,4	1,8

Figure C.2. Optimal parameters for the T-ECMS strategy.

### C.0.1 Defining the range of the parameters

It is important to choose the step-size and range of the parameters wisely before the tuning is begun, while the amount of simulations increases drastically with the increasing amount of values in the range and possible combinations between them. In case of the T-ECMS algorithm the range was set to lie around the balancing value of the equivalence factor given in equation 5.16. Values of  $S_{dis}$  or  $S_{chg}$  that are too far from the balancing value of the equivalence factor will result in poor behavior of the torque-split control within the EECU. If the parameter values are much lower than the balance factor given in equation 5.16 then also the resulting equivalence factor will have low values which means that the cost of using electric energy is low

Battery capacity	MDS	Drive cycle	$s_0$	k
1350 Wh	120 kW	BLB	2,1	0,2
		PL	1,4	0,2
		sx135	1,7	0,1
	60 kW	BLB	2,2	0,3
		PL	2,1	0,1
		sx135	1,7	0,1
600 Wh	120 kW	BLB	1,9	0,2
		PL	1,4	0,2
		sx135	1,7	0,1
	60 kW	BLB	2,1	0,1
		PL	2,0	0,1
		sx135	1,8	0,1

Figure C.3. Optimal parameters for the pRSG strategy.

and the optimal control law from equation 5.12 will be to distribute full torque from the EM at all times. This strategy will just use the stored electric energy as fast as possible and will not take benefit from any predictive information, as can be seen in figure C.4. If on the other hand the values for  $S_{dis}$  and  $S_{chg}$  are much higher than the balance factor the resulting equivalence factor will also have a high value which will result in a control law that neglects the use of electric energy leading to an underused hybrid system, which can be seen in figure C.5.

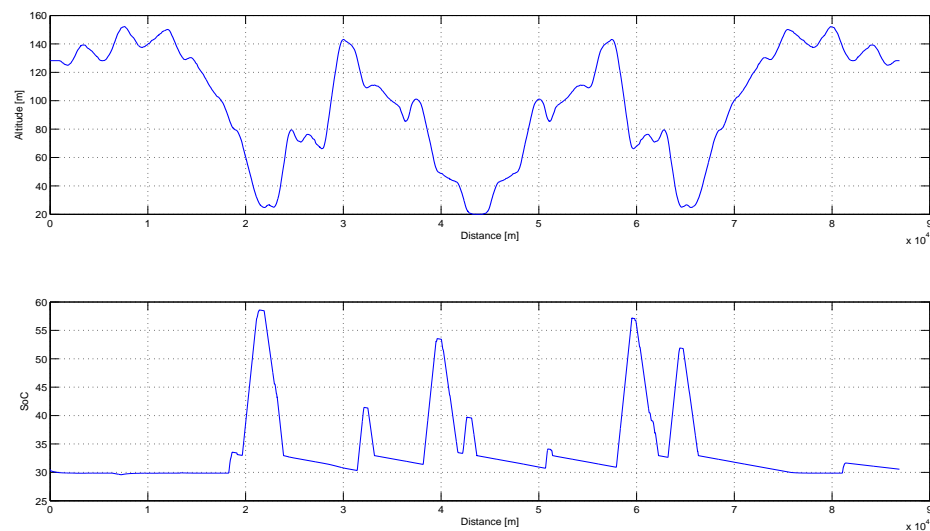


Figure C.4. SoC-curve over the BLB drive-cycle with the T-ECMS strategy. Parameters are much lower than the balancing factor of the equivalence factor.

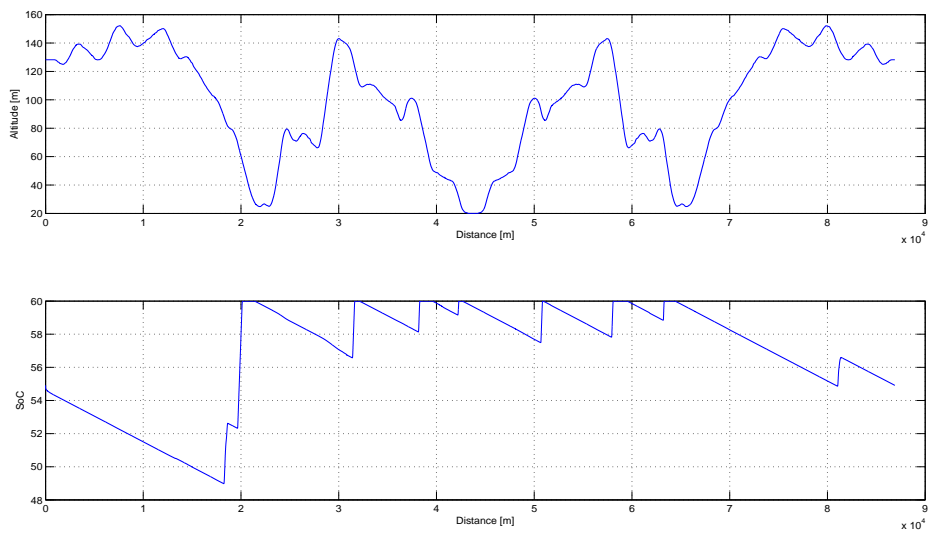


Figure C.5. SoC-curve over the BLB drive-cycle with the T-ECMS strategy. Parameters are much higher than the balancing factor of the equivalence factor.

# Appendix D

## Drive cycles

app:drivecycles

Three drive cycles were chosen for simulations. One important factor for these drive cycles is the average road gradient which describes how hilly each drive cycle is on average. The higher the road gradient, the hillier the road. In previous simulations at Volvo it has been shown that there is a correlation between the average road gradient and the fuel saving for an HEV and that the correlation is not linear due to saturations in the hybrid systems. The hybrid system can only recuperate a given maximal amount of energy due to the power-flow limitations within the generator and the EES. For low average gradients the battery never gets fully charged and the hybrid system is underused, and for high average gradients the brake-power may exceed the power intake of the generator or the ESS may get fully charged and saturated. The three drive cycles were chosen to represent a variety of average road gradients. Below follows some information about these drive cycles.

Borås-Landvetter-Borås (BLB) Predominately flat, 0 stops, target speed 90 km/h  
Average gradient: 1.23 % Length 87 km

Paris-Lille (PL) Flat, 0 stops, target speed 90 km/h Average gradient: 0.78 %  
Length 29 km

Frankfurt-Koblenz (SX135) Hilly, 0 stops, target speed 85 km/h Average gradient:  
1.44 % Length 210 km

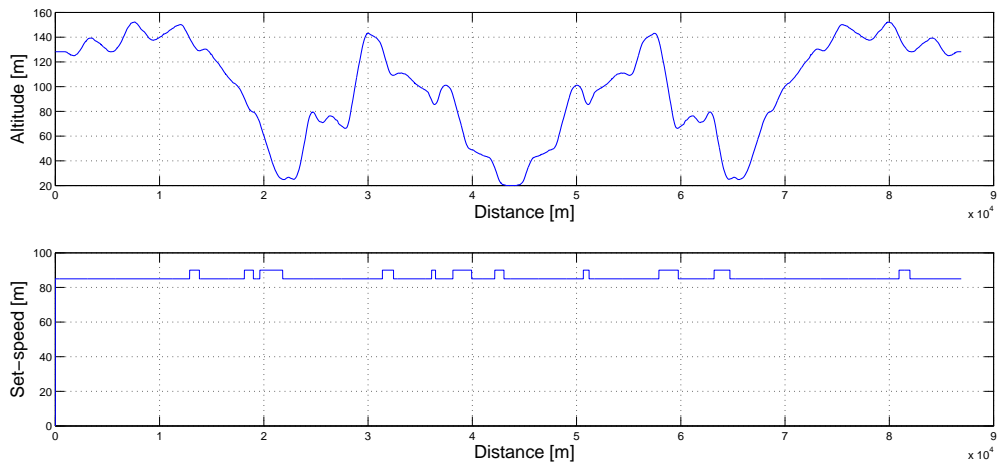


Figure D.1. Altitude and set-speed for the Borås-Landvetter-Borås (BLB) drive cycle.

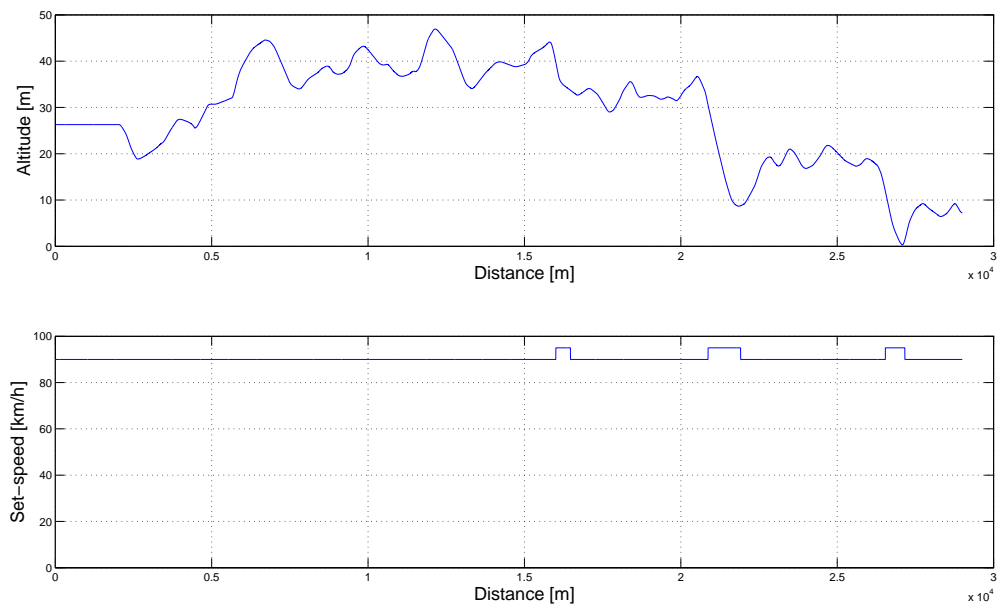


Figure D.2. Altitude and set-speed for the Paris-Lille (PL) drive cycle.

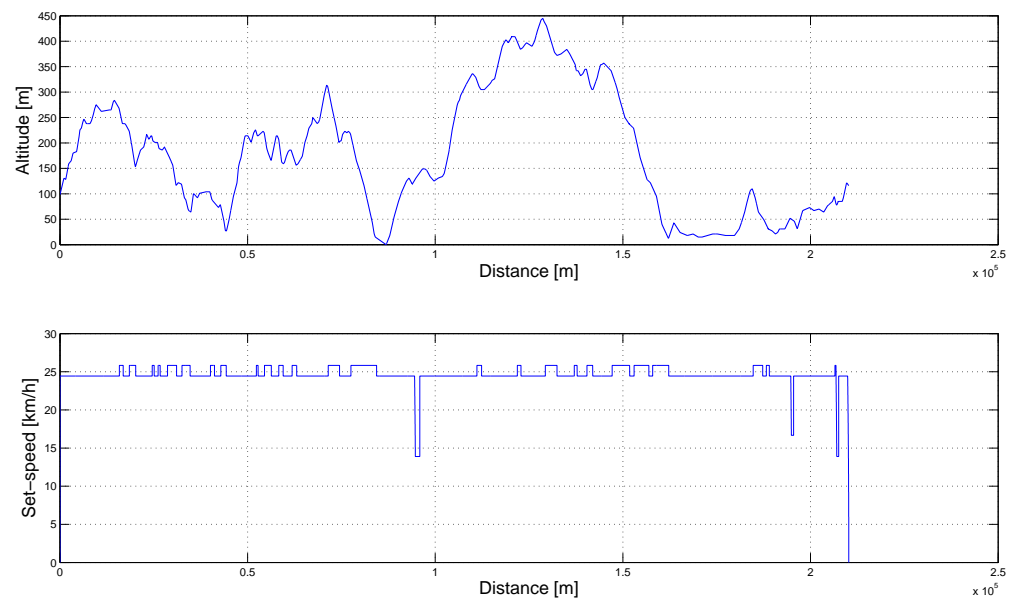


Figure D.3. Altitude and set-speed for the Frankfurt-Koblenz (sx135) drive cycle.



# Appendix E

## Series hybrid

sec:serieshybrid

In a series hybrid electric vehicle the EM delivers all the energy to the wheels, and thus alone propels the vehicle. The electric energy needed can come from a battery, an engine-propelled generator or both. Engine-propelled generators are used because driving on only electric energy is not sufficient when longer driving distances are desired. This is due to the much smaller efficiency of batteries as energy storage devices compared to fuel based energy storages, as can be seen in figure 4.2. The energy output from the engine is then not related to the energy demand of the vehicle and therefore the engine can be run at an optimal operating point at all times when recharging the battery [19]. The electric motor has to be designed so that it can meet the power demands of the vehicle.

The energy produced by the engine-generator pair can directly be used by the electric motor or be saved in the battery for later use. During regeneration the traction motor is used as a generator. Schematic of the series hybrid configuration is given in figure E.

The advantage of a series hybrid is that the transmission does not need a clutch because the engine is disengaged from the powertrain. The disadvantage is that the series hybrid needs three machines; one engine, one electric motor and one generator.

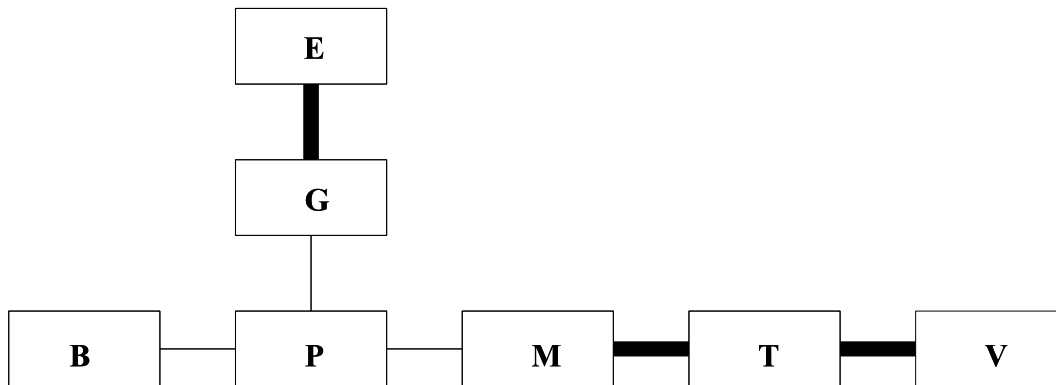


Figure E.1. Basic series hybrid configuration. B: battery, E: engine, G: generator, M: motor, P: power converter, T: transmission (including clutch and gears), V: axles and vehicle. Bold lines: mechanical link, solid lines: electrical link.